

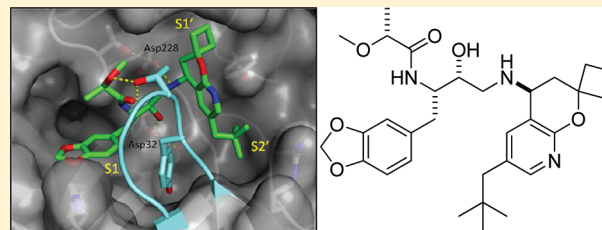
Design and Preparation of a Potent Series of Hydroxyethylamine Containing β -Secretase Inhibitors That Demonstrate Robust Reduction of Central β -Amyloid

Matthew M. Weiss,^{*,†} Toni Williamson,[‡] Safura Babu-Khan,[§] Michael D. Bartberger,^{||} James Brown,[†] Kui Chen,[§] Yuan Cheng,[†] Martin Citron,^{‡,#} Michael D. Croghan,[†] Thomas A. Dineen,[†] Joel Esmay,[⊥] Russell F. Graceffa,[†] Scott S. Harried,[†] Dean Hickman,[⊥] Stephen A. Hitchcock,^{†,▽} Daniel B. Horne,[†] Hongbing Huang,[†] Ronke Imbeah-Ampiah,[†] Ted Judd,[†] Matthew R. Kaller,[†] Charles R. Kreiman,[†] Daniel S. La,[†] Vivian Li,^{||} Patricia Lopez,[†] Steven Louie,[⊥] Holger Monenschein,^{†,▽} Thomas T. Nguyen,[†] Lewis D. Pennington,[†] Claire Rattan,[‡] Tisha San Miguel,[§] E.Allen Sickmier,^{||} Robert C. Wahl,[§] Paul H. Wen,[‡] Stephen Wood,[‡] Qiufen Xue,[†] Bryant H. Yang,[†] Vinod F. Patel,^{†,○} and Wenge Zhong[†]

[†]Departments of Chemistry Research and Discovery, [‡]Neuroscience, [§]HTS Molecular Pharmacology, ^{||}Molecular Structure, [⊥]Pharmacokinetics and Drug Metabolism, Amgen Inc., 360 Binney Street, Cambridge, Massachusetts 02142, United States, and One Amgen Center Drive, Thousand Oaks, California 91320, United States

S Supporting Information

ABSTRACT: A series of potent hydroxyethyl amine (HEA) derived inhibitors of β -site APP cleaving enzyme (BACE1) was optimized to address suboptimal pharmacokinetics and poor CNS partitioning. This work identified a series of benzodioxolane analogues that possessed improved metabolic stability and increased oral bioavailability. Subsequent efforts focused on improving CNS exposure by limiting susceptibility to Pgp-mediated efflux and identified an inhibitor which demonstrated robust and sustained reduction of CNS β -amyloid ($A\beta$) in Sprague–Dawley rats following oral administration.



■ INTRODUCTION

Alzheimer's disease (AD) is a progressive neurodegenerative disorder that is currently the leading cause of dementia in the elderly and as such represents a major unmet medical need.¹ Despite the devastating effects of this disease, therapeutic options for treating AD remain limited. Current treatments have no disease modifying effect and are approved only for the management of the symptoms associated with the disease.²

There is a compelling amount of data, both histopathological and genetic, suggesting that the mis-metabolism of amyloid precursor protein (APP) and the formation of β -amyloid ($A\beta$) peptides play an early and critical event in the pathogenesis of AD.³ These $A\beta$ peptides, particularly $A\beta_{40-42}$, subsequently aggregate and lead to one of the key hallmarks of AD, β -amyloid plaques. While the specific role of these plaques in the progression of the disease is unclear, one of the key therapeutic approaches to treat AD relies on the ability to inhibit the formation of $A\beta$ peptides. To this end, it is generally recognized that the formation of these $A\beta$ peptides is achieved by the sequential proteolytic activity of β - and γ -secretases, the former being rate-limiting.⁴ Thus, inhibition of β -site amyloid precursor protein cleaving enzyme (BACE1) is seen as an attractive therapeutic target for the treatment and prevention of AD.^{5,6} Herein we report the identification of a series of

hydroxyethyl amine (HEA)-containing BACE1 inhibitors that demonstrate robust reduction of central $A\beta$ in a rodent pharmacodynamic model following oral dosing.

Previous work from our laboratories led to the identification of a potent and highly efficient class of HEA BACE1 inhibitors.⁷ This series, exemplified by **1**, utilized a highly substituted azachroman amine to access the lipophilic S1' and S2' pockets of the BACE1 enzyme while leaving the S2 and S3 pockets largely unoccupied (Figure 1, Table 1). While this series exhibited potent cellular inhibition of the BACE1 enzyme, the majority of compounds within this series demonstrated poor metabolic stability and suboptimal pharmacokinetics (i.e., high CL, low bioavailability). In the course of SAR studies, it was found that the inclusion of a *para*-fluoro phenyl P1 moiety gave rise to an inhibitor (**2**) with a uniquely improved pharmacokinetic profile relative to its congeners. This compound, which demonstrated reduced turnover in both rat and human liver microsomes, also exhibited reduced *in vivo* clearance. Oral administration of **2**

Special Issue: Alzheimer's Disease

Received: January 27, 2012

Published: April 2, 2012

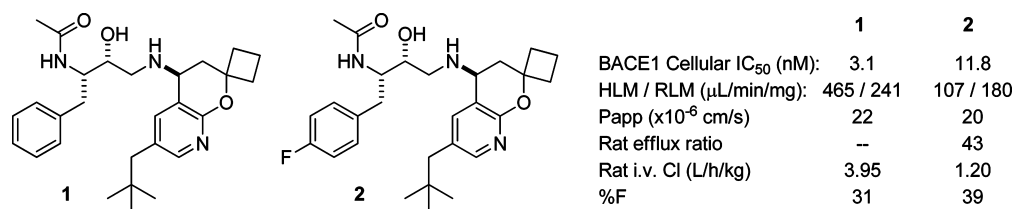


Figure 1. Previously reported BACE1 inhibitors.

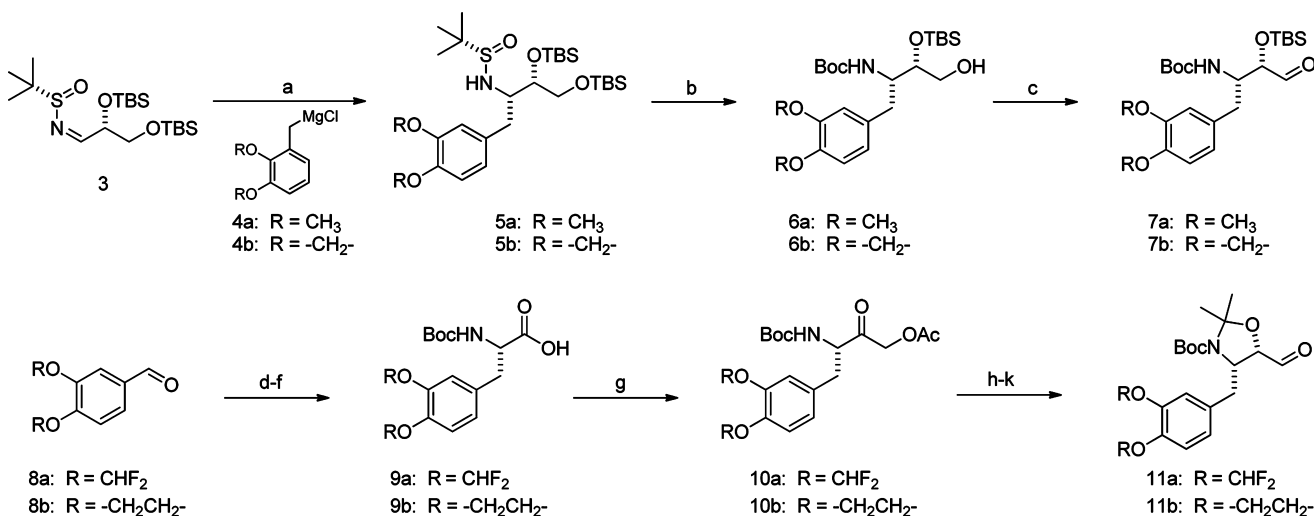
Table 1. BACE1 SAR, in Vitro Metabolic Stability, Rat Pharmacokinetics, and Pgp Transport Properties

Cpd ^a	P1	BACE1 IC ₅₀ (nM) ^{b,c}	Cellular IC ₅₀ (nM) ^b	HLM / RLM (μL/min/mg) ^d	Cl (L/hr/kg) ^e	F (%)	Papp (x10 ⁻⁶ cm/s) ⁱ	Human Efflux ratio ^{ij}	Rat Efflux ratio ^{ij}
1		5.8	3.1	465 / 241	3.95	31 ^f	22	12	NA
2		5.0	11.8	107 / 180	1.20	39 ^g	20	18	43
15		18.2	9.3	103 / 119	4.46	NA	21	34	>50
16		35.2	238.4	590 / 143	NA	NA	8	>50	>50
17		8.0	5.5	19 / 132	1.05	97 ^h	11	19	49
18		22.8	22.9	356 / 447	NA	NA	20	36	20

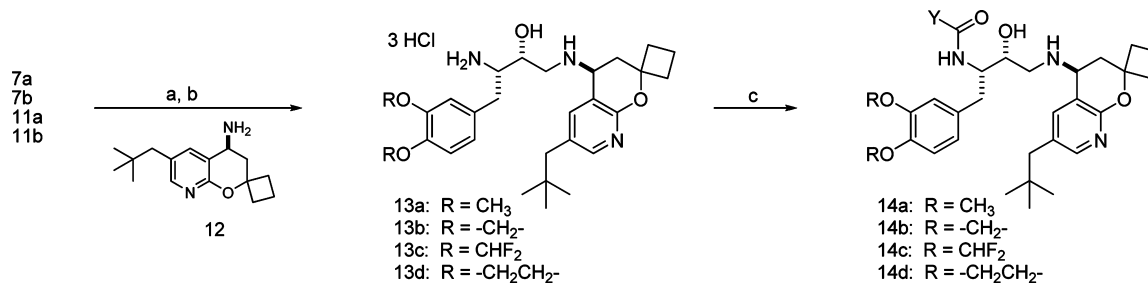
^aCompounds were >95% pure by ¹H NMR and HPLC. ^bValues represent the mean of at least two experiments. ^cBiochemical IC₅₀. ^dCompounds are incubated with microsomes for 30 min at a concentration of 1 μM. ^e2 mg/kg iv dose (solution in 100% DMSO). ^f5 mg/kg oral dose (solution in 1% Tween/2%HPMC). ^g2 mg/kg oral dose (solution in 1% Tween/2%HPMC). ^h10 mg/kg oral dose (solution in 1% Tween/2%HPMC). ⁱParental LLC-PK1 cell line. ^jB/A–A/B ratio.

to Sprague–Dawley rats at 100 mg/kg resulted in modest reduction of both CSF and brain Aβ levels (35% and 32%, respectively). These pharmacodynamic effects were measured 4 h post dose and occurred with drug exposures of: [plasma]_{unbound} = 64 nM and [CSF] = 6 nM. Given the potent nature of this compound in our functional BACE1 assay, the modest pharmacodynamic effect observed was attributed to suboptimal pharmacokinetics and poor CNS penetration. Indeed, systemic exposure was limited by moderate to high clearance and low oral bioavailability. In addition, brain exposure was restricted by Pgp-mediated efflux, even while the passive permeability was shown to be excellent. Efforts to

further improve the metabolic stability of related compounds were met with little success, as this series was predisposed to high metabolic turnover. In this communication, we describe the development of a related series of potent BACE1 inhibitors which demonstrate robust reduction of central Aβ following oral dosing in naïve rats. This series addresses the two dominant barriers that have limited the utility of the HEA scaffold as a template for the development of BACE1 inhibitors: poor metabolic stability and a high susceptibility to Pgp-mediated efflux.

Scheme 1^a

^a(a) THF, -65 °C, 42–76%; (b) HCl, ethanol 15 °C then Boc₂O, TEA, 73–78%; (c) Dess–Martin periodinane, NaHCO₃, CH₂Cl₂, 72–91%; (d) methyl 2-(*tert*-butoxycarbonylamino)-2-(dimethoxyphosphoryl)acetate, DBU, DCM, 65–94%; (e) (1*R*,1*R'*,2*S*,2*S'*)-(COD)Rh(DuanPhos)BF₄, CH₃OH, H₂, 50 psi, 94–96%, >95% ee; (f) LiOH, THF, H₂O, 100%; (g) isobutyl chloroformate, TEA, CH₂N₂, THF/HBr, AcOH, THF; K₂CO₃, NaOAc, DMF, 42–99%; (h) LiH(OtBu)₃, THF, -78 °C, 82–98%; (i) dimethoxypropane, CSA, DMF, 95–96%; (j) K₂CO₃, CH₃OH, 50–74%; (k) Dess–Martin periodinane, NaHCO₃, CH₂Cl₂, 84–93%.

Scheme 2^a

^a(a) 12, (CH₃O)₃CH, NaBH(OAc)₃, CH₂Cl₂; (b) HCl, dioxane, CH₃OH, 97–100%, 2 steps; (c) *N*-acetylimidazole, DIPEA, DMF, 39–72%, or carbonyldiimidazole, DIPEA, Y-CO₂H, CH₂Cl₂, 77–91%, or HATU, Y-CO₂H, DIPEA, DMF, 35–53%.

CHEMISTRY

Compounds 15–26 were prepared using the routes illustrated in Schemes 1 and 2. The key aldehyde building blocks (7a,b and 11a,b) were constructed using the protocols shown in Scheme 1. The coupling of either 3,4-dimethoxybenzyl magnesium chloride (4a) or (benzo[*d*][1,3]dioxol-4-ylmethyl)magnesium chloride (4b) with sulfonimine 3 proceeded with a moderate level of diastereoselectivity (84–91% de) to provide adducts 5a–b in good overall yield.⁸ Simultaneous unmasking of the amine and primary alcohol was achieved by exposure to HCl in cold ethanol. Protection of the derived amines provided carbamates 6a–b which were subsequently oxidized to furnish aldehydes 7a–b. Aldehydes 11a–b were accessed via an alternative route that commenced with the homologation of 8a–b with methyl 2-(*tert*-butoxycarbonylamino)-2-(dimethoxyphosphoryl)acetate. The derived enone products underwent an enantioselective 1,4-reduction mediated by (1*R*,1*R'*,2*S*,2*S'*)-Rh(DuanPhos) to furnish esters that were subsequently saponified to provide amino acids 9a–b in high yield and enantiopurity. A one carbon homologation with diazomethane followed by sequential treatment with HBr in acetic acid and sodium acetate provided acetoxy ketones 10a–b. A substrate directed reduction with lithium *tert*-butoxy-

hydride followed by protection of the resulting vicinal amino alcohol provided the corresponding *N,O*-acetonides. Finally, deprotection of the acetate and oxidation of the primary alcohol with Dess–Martin periodinane furnished aldehydes 11a–b.

Aldehydes 7a–b and 11a–b were advanced by the route illustrated in Scheme 2. Reductive amination with azachromanamine 12 followed by global deprotection provided hydroxyethyl amines 13a–d.^{6,7} Finally, acylation furnished inhibitors of type 14a–d.

RESULTS AND DISCUSSION

In an effort to identify BACE1 inhibitors with improved pharmacokinetic parameters, a series of inhibitors related to 2 but with alternatively substituted aryl P1 fragments were prepared and examined. Compounds were initially surveyed based on potency against the BACE1 enzyme in an enzymatic and cellular format, turnover in rat and human liver microsomes, passive permeability, and the potential for human (MDR1) and rat (*mdr1a*) Pgp-mediated efflux. Compounds that demonstrated low to moderate turnover upon incubation with microsomes were further evaluated in vivo.

Table 2. In Vivo $A\beta_{40}$ Reduction in Naïve Rats at 4 h with 17 (30 mg/kg, po)

compd	dose (mg/kg) ^a	cellular IC ₅₀ (nM)	[plasma] _{total} (μ M)	[plasma] _{unbound} (μ M)	[brain] (μ M)	[CSF] (μ M)	CSF $A\beta_{40}$ reduction (%)
17	30	5.5	9.61	0.374	0.750	0.022	52

^aDosed as a solution in mg/kg oral dose (solution in 1% Tween/2%HPMC).

Upon confirmation that the metabolic fate of compound 1 (and related compounds) was largely oxidative in nature, attention shifted to improving the intrinsic stability of this series of inhibitors. Efforts to improve metabolic stability by blocking the primary sites of metabolism proved unsuccessful, so attention turned to reducing the overall lipophilicity of the inhibitors, a well-known strategy to reduce the affinity of any given molecule toward members of the cytochrome P-450 (Cyp) family.^{9,10} This work led to the identification of compound 15, an inhibitor containing a dimethoxyphenyl group in P1. In relation to 1, 15 exhibited a slight loss in potency against the BACE1 enzyme but lacked a shift between enzyme and cell IC₅₀s and maintained an IC₅₀ of less than 10 nM in the functional cell-based assay. More importantly, the increased polarity of 15 did indeed translate to improved stability in the presence of human and rat liver microsomes; however, following iv administration, 15 exhibited high in vivo clearance. Intrigued by the favorable profile of 15 in the presence of microsomes, a number of related analogues that contained a high degree of oxygenation in P1 were prepared and surveyed. Related analogues containing a bis-(difluoromethoxy)benzyl unit (16) or a dihydrobenzo[*b*][1,4]-dioxine moiety (18) in P1 showed a moderate loss in inhibitory activity and exhibited high intrinsic clearance in human and/or rat liver microsomes, however, 17, containing a benzo[*d*][1,3]-dioxole, exhibited an overall improved profile. Compound 17 maintained BACE1 potency, exhibited low to moderate turnover in microsomes, and was subsequently found to demonstrate moderate in vivo clearance and excellent bioavailability (Table 2). To better understand the dramatic enhancement in the metabolic stability of 17 in the presence of human liver microsomes, a number of Cyp inhibition studies were performed and it was found that this compound demonstrated potent inhibition of Cyp 3A4 (96% at 1 μ M).¹¹ It is well established that the benzodioxole group can complex with the heme function of Cyp isozymes through a carbene metabolite.¹² While it is important to note that inhibition of Cyp 3A4 can potentially result in drug–drug interactions, there is a substantial amount of clinical data within the field of HIV protease inhibitors wherein this has been shown to be manageable.¹³ Furthermore, most currently prescribed HIV protease inhibitors are coadministered with the potent Cyp 3A4 inhibitor ritonavir. This boosted protease inhibitor regimen serves to enhance the overall exposure of the protease inhibitor that is concomitantly administered with ritonavir.¹⁴ The resultant increases in the AUC, C_{max} and *t*_{1/2} thereby lead to improved efficacy of the second protease inhibitor. Given the utility of this approach within the field of a chronically managed, protease-mediated disease state, we opted to pursue a similar strategy wherein the Cyp inhibition element would be incorporated within the framework of our BACE1 inhibitors.¹⁵

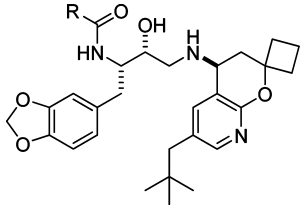
While 17 showed potent inhibition of the BACE1 enzyme and demonstrated improved pharmacokinetic parameters, it also proved to be an excellent substrate for Pgp-mediated efflux. There is a wealth of literature supporting the notion that

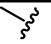
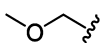
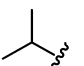
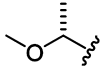
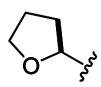
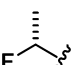
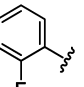
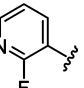
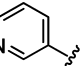
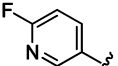
penetration across the blood–brain barrier (BBB) and into the CNS is substantially reduced for compounds which demonstrate low passive permeability and a high potential for Pgp-mediated efflux in vitro.¹⁶ This phenomenon held true when 17 was examined for its ability to acutely reduce CSF $A\beta_{40}$ levels in vivo. Toward this end, Sprague–Dawley rats were orally administered 17 and CSF $A\beta_{40}$ levels were measured 4 h post dose. As illustrated in Table 2, a single 30 mg/kg dose of 17 provided a 52% reduction in CSF $A\beta_{40}$ levels. While this level of CSF $A\beta_{40}$ reduction was encouraging, the low brain to plasma ratio (<0.1) and, more importantly, the large disparity between unbound plasma drug levels and drug levels in the CSF highlighted the need to mitigate the potential for Pgp-mediated efflux. CSF drug levels were used as a surrogate marker for the unbound drug in the CNS, and a strong PK/PD relationship was observed within this series. In particular, it was demonstrated that robust CSF $A\beta_{40}$ reduction was only observed when drug levels in the CSF exceeded the cellular IC₅₀.¹⁷ The poor CNS partitioning of 17, likely a reflection of its susceptibility to Pgp-mediated efflux, thus required exceedingly high plasma drug levels ([plasma]_{total} = 9.61 μ M and [plasma]_{unbound} = 0.374 μ M) in order to elicit a pharmacodynamic effect. This in turn has the potential to reduce the therapeutic window of an agent, as higher unbound plasma concentrations are required to compensate for the active transport out of the CNS.

In light of the above-mentioned findings, subsequent optimization efforts within this series focused on a rational approach to mask Pgp recognition elements. Several strategies have been successfully utilized by medicinal chemists to influence the CNS penetration of small molecules by modulating active transport.¹⁸ We ultimately pursued a strategy wherein hydrogen bond donors contained within 17 were masked either by the introduction of flanking groups or intramolecular hydrogen bonds.¹⁹ Given the crucial binding interactions between the catalytic aspartates of the BACE1 enzyme and the alcohol and the secondary amine of the inhibitors (vide infra), efforts focused on masking the hydrogen bond donor contained within the amide functionality.

To this end, introduction of a 2-methoxyamide (19) provided a compound which maintained BACE1 potency, albeit with a slightly increased enzyme to cell shift. This compound, which has the ability to form an intramolecular hydrogen bond between the ethereal oxygen and the amide N–H, demonstrated only a slightly improved efflux ratio when compared to parent acetamide 15. Alternatively, isobutyramide 20 was prepared to gauge the effect of simply increasing the steric bulk around the amide. Interestingly, while this compound showed a considerably reduced susceptibility to Pgp-mediated efflux, it also showed a substantial loss in potency against the BACE1 enzyme. In an effort to merge the potency of methoxyacetamide 19 with the beneficial efflux characteristics of isobutyramide 20, compounds 21 and 22 were targeted. These compounds incorporated the ethereal oxygen of 19 with the additional steric bulk found in 20. Both 21 and 22 showed a slight loss in potency against the BACE1 enzyme

Table 3. BACE1 SAR, in Vitro Metabolic Stability, Rat Pharmacokinetics, and Pgp Transport Properties



Cpd ^a	R	BACE1 IC ₅₀ (nM) ^{b,c}	Cellular IC ₅₀ (nM) ^b	HLM / RLM (μL/min/mg) ^d	Papp (x10 ⁻⁶ cm/s) ^e	Human Efflux ratio ^{e,f}	Rat Efflux ratio ^{e,f}
15		8.0	5.5	19 / 132	11	19	49
19		5.4	16.8	19 / 140	17	16	27
20		144	812	31 / 110	17	5	11
21		16.8	26.0	25 / 151	23	4	6
22		20.4	27.5	36 / 166	19	5	6
23		28.9	55.5	42 / 114	16	2	4
24		76.6	1,150	-- / --	11	1	1
25		33.2	64.3	49 / 165	17	4	2
26		26.1	67.6	39 / 95	11	49	39
27		48.4	69.5	36 / 93	18	35	34

^aCompounds were >95% pure by ¹H NMR and HPLC. ^bValues represent the mean of at least two experiments. ^cBiochemical IC₅₀. ^dCompounds are incubation with microsomes for 30 min at a concentration of 1 μM. ^eParental LLC-PK1 cell line. ^fB/A–A/B ratio.

but exhibited considerably improved efflux ratios relative to **15**. Similar results could be obtained by replacing the ethereal oxygen in the amide tether with a fluorine atom (e.g., **23**). Compound **23** also showed a reduced potential for Pgp-mediated efflux; however, the increased hydrophobic nature of this inhibitor led to a slightly higher enzyme to cell shift. It is believed that the mitigated efflux of **19–23** results from an increase in steric bulk around the amide as well as a partial masking of the amide N–H by intramolecular hydrogen bonding. Pgp recognition could be eliminated by incorporating an *ortho*-fluoro substituted arylamide (**24**). While this

compound showed no potential for efflux, it did show reduced potency against BACE1 and a very large enzyme to cell IC₅₀ shift. Introduction of a heteroatom into the aryl ring (**25**) served to reduce the enzyme to cell IC₅₀ shift while maintaining a low efflux ratio, yet **25** remained considerably less potent than **15**. To gauge whether the reduced efflux of aryl amides **24** and **25** was a result of steric congestion or hydrogen bonding, aryl amide **26** (which lacks the ability to hydrogen bond with the amide N–H) was prepared. Compound **26** demonstrated high efflux, suggesting that the reduced efflux of **24** and **25** results from intramolecular hydrogen bonding between the aryl

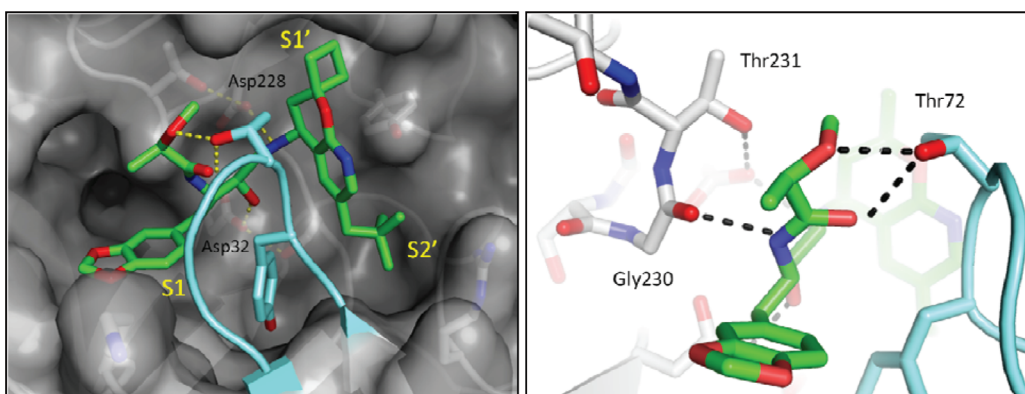


Figure 2. Cocrystal structure of BACE1 complexed with **21**; the flap is depicted in blue. (left) Interactions in S1' and S2' as well as the hydrogen bonding between **21** and the catalytic aspartates. (right) Hydrogen bonding contacts between Gly230 and Thr72 residues and the amide of **21**.

fluoride and the amide N–H. Furthermore, compound **27**, a constitutional isomer of **25** which lacks an appropriately positioned fluorine atom to mask the amide N–H, demonstrated a high potential for efflux, further supporting the suggestion that the observed reduction in efflux with compounds **21**–**25** is indeed related to masking of the amide N–H and is not simply due to a modulation of overall polarity (i.e., PSA). In general, all of the compounds in Table 3 demonstrated low turnover in human liver microsomes and moderate turnover in rat liver microsomes. Furthermore, with the exception of **15** and aryl amides **24** and **26**, all of the compounds in Table 3 demonstrated improved passive permeability ($>15 \times 10^{-6}$ cm/s).

Intrigued by the disparity in potency exhibited by isobutyramide **20** and (*R*)-2-methoxypropanamide **21**, we obtained an X-ray cocrystal of **21** and the BACE1 enzyme (Figure 2).²⁰ As anticipated, this compound resides in the active site of the enzyme with the benzodioxolane ring system occupying S1 and the hydroxyl group and secondary amine each engaging one of the catalytic aspartates (Asp32 and Asp228). The spirocyclobutane ring and the neopentyl group flanking the azachroman ring system occupy S1' and S2', respectively. Inspection of the acetamide region of the molecule reveals that the amide N–H is interacting with Gly230 while the carbonyl and methoxy group are engaging Thr72 in a bidentate manner. This latter interaction between Thr72, a residue in the flap region of the BACE1 enzyme, and the methoxy group explains the considerable loss in potency that is observed in going from **21** to **20**.²¹ The three residues Gly230, Thr231, and Thr72 form a relatively small pocket that prefers branched acetamides containing a hydrogen bond acceptor to interact with Thr72.

As a result of their potent inhibition of BACE1, moderate turnover in rat liver microsomes and improved efflux parameters, compounds **21** and **23** were further profiled in vivo (Table 4). Both compounds showed moderate clearance,

Table 4. Pharmacokinetic and In Vitro Parameters for BACE1 Inhibitors **21** and **23** in Rat

compd	Cl ^a (L/h/kg)	V _{dss} ^a (L/kg)	t _{1/2} ^b (h)	C _{max} ^b (μM)	t _{max} ^b (h)	%F ^b
21	0.465	12.3	2.98	3.56	1.83	130
23	0.448	23.9	4.64	3.80	4.67	39

^a2 mg/kg iv dose (solution in 100% DMSO). ^b5 mg/kg oral dose (solution in 1% Tween/2%HPMC).

high V_{dss} and half-lives of ~3–5 h. Where the compounds differed was in oral bioavailability, with **21** being >100% and **23** being a much more modest 39%.

Given its superior bioavailability in rats, a more extensive pharmacokinetic profile of **21** across dogs and rhesus monkeys was obtained (Table 5). Compound **21** exhibited low to

Table 5. Beagle Dog and Rhesus Pharmacokinetics for **21**

compd	beagle dog PK			rhesus PK		
	Cl ^a (L/h/kg)	V _{dss} ^a (L/kg)	t _{1/2} ^b (h)	Cl ^a (L/h/kg)	V _{dss} ^a (L/kg)	t _{1/2} ^b (h)
21	0.393	1.03	9.77	1.65	1.46	1.74

^a2 mg/kg iv dose (solution in 5%propylene glycol/95%dextrose). ^b10 mg/kg oral dose (solution in 5%propylene glycol/95%dextrose).

moderate clearance in beagle dogs and elevated clearance in rhesus monkeys. In contrast to the profile observed in rats, low V_{dss} was seen in both species. This profile led to an extended half-life in dogs (~10 h) and a relatively short half-life in rhesus monkeys (<2 h).

On the basis of its pharmacokinetic profile, compound **21** was advanced to an in vivo study to examine its ability to reduce Aβ₄₀ levels in both the peripheral and central compartments. This study incorporated doses of 10, 30, and 100 mg/kg and included a number of time points to gain insight on the temporal component to Aβ₄₀ lowering. Compound **21** was orally administered to Sprague–Dawley rats, and Aβ₄₀ levels were measured 4 h postdose (Table 6; Figure 3). A dose- and exposure-dependent decrease in Aβ₄₀ levels (10, 30, and 100 mg/kg) was observed in plasma, CSF, and brain. At the 4 h time point, substantial Aβ₄₀ reduction was observed peripherally but not centrally following a 10 mg/kg dose. However, at the same time point, a 30 mg/kg dose led to substantial drug levels in the CNS (brain, 1.02 μM; CSF, 0.114 μM) and a significant reduction in Aβ₄₀ in both the brain (44%) and CSF (61%). Furthermore, the large disparity previously observed between the unbound plasma and CSF drug levels following oral dosing of **17** (17-fold) was significantly reduced upon administration of **21** (<3-fold). The unbound plasma levels of **21** more closely resembled the measured CSF drug levels, demonstrating that the optimization of efflux in vitro was a useful means by which to improve brain penetration. Compound **21** was also examined in a time course study wherein Aβ₄₀ levels were measured at 4, 8, 16, and 24 h following a 100 mg/kg oral dose. As illustrated in Table 6 and

Table 6. In Vivo $A\beta_{40}$ Reduction in Naïve Rats with 21 (10, 30, and 100 mg/kg, po)

dose (mg/kg) ^a	time (h)	[plasma] _{total} (μ M)	[plasma] _{unbound} ^b (μ M)	[brain] (μ M)	[CSF] (μ M)	plasma $A\beta_{40}$ reduction (%)	CSF $A\beta_{40}$ reduction (%)	brain $A\beta_{40}$ reduction (%)
10	4	1.85	0.019	0.617	0.008	59	21	14
30	4	8.15	0.305	1.02	0.114	67	61	44
100	4	16.2	1.12	3.44	0.563	75	77	68
100	8	15.3	1.03	3.24	0.477	68	78	63
100	16	3.05	0.057	0.829	0.056	50	32	9
100	24	0.705	0.006	0.571	BQ	35	15	12

^aDosed as a solution in mg/kg oral dose (solution in 1% Tween/2%HPMC). ^bSaturable plasma protein binding was observed over the range of 1–100 μ M.²²

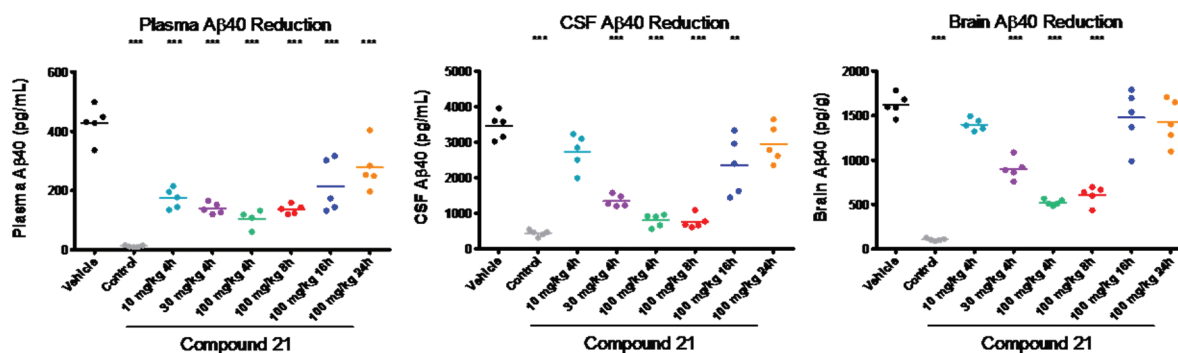


Figure 3. In vivo $A\beta_{40}$ reduction in naïve rats with 21 (10, 30, and 100 mg/kg, po). *** $P \leq 0.0001$; ** $P \leq 0.005$.

Figure 3, 21 showed robust and sustained reduction of $A\beta_{40}$ levels in all compartments for at least 8 h. $A\beta_{40}$ levels in the CSF and brain returned to baseline after 16 h. The data in Table 6 exemplify the PK/PD relationship observed between CNS $A\beta_{40}$ reduction and CSF drug levels. Notably, the improved distribution of 21 into the CNS (relative to 17) serves to effectively increase the therapeutic window by reducing the systemic exposure required to achieve appropriate CNS drug levels. Efforts to further optimize this series of inhibitors are the subject of the companion paper.³²

CONCLUSION

In conclusion, a series of potent BACE1 inhibitors have been optimized to improve pharmacokinetic properties and enhance penetration into the CNS. This work began by introducing polar functionality to improve metabolic stability and identification of a series of benzodioxolones with improved clearance and bioavailability. This utilized a strategy wherein overall plasma exposure was boosted by inhibition of Cyp 3A4. Subsequent efforts focused on improving brain uptake. This was successfully accomplished by strategically introducing functional elements to mitigate Pgp-mediated efflux. Compound 21 demonstrated robust and dose dependent CNS $A\beta_{40}$ reduction and has served as a key stepping stone for future efforts. This work highlights the importance of optimizing across multiple parameters, in this case at the expense of potency, when trying to identify centrally active agents.

EXPERIMENTAL SECTION

BACE1 Enzymatic Assay. BACE1 enzymatic activity was determined by the enhancement of fluorescence intensity upon enzymatic cleavage of the fluorescence resonance energy transfer substrate. The BACE1 recognition and cleavage sequence of the substrate is derived from the reported literature,²³ and the fluorophore and quencher dyes are attached to side chain of Lys residues at the termini of the substrate peptide. The human recombinant BACE1²⁴

assay was performed in 50 mM acetate, pH 4.5/8% DMSO/100 μ M Genapol/0.002% Brij-35. In dose–response IC_{50} assays, 10 point 1:3 serial dilutions of compound in DMSO were preincubated with the enzyme for 60 min at room temperature. Subsequently, the substrate was added to initiate the reaction. After 60 min at room temperature, the reaction was stopped by addition of 0.1 M Tris base to raise the pH above the enzyme active range and the increase of fluorescence intensity was measured on Safire II microplate reader (Tecan, Männedorf, Switzerland).

Cell-Based Assay. Human embryonic kidney cells (HEK293) stably expressing APP_{SW} were plated at a density of 100K cells/well in 96-well plates (Costar). The cells were cultivated for 6 h at 37 °C and 5% CO₂ in DMEM supplemented with 10% FBS. Cells were incubated overnight with test compounds at concentrations ranging from 0.0005 to 10 μ M. Following incubation with the test compounds, the conditioned media was collected and the $A\beta_{40}$ levels were determined using a sandwich ELISA. The IC_{50} was calculated from the percent of control $A\beta_{40}$ as a function of the concentration of the test compound. The sandwich ELISA to detect $A\beta_{40}$ was performed in 96-well microtiter plates, which were precoated with goat antirabbit IgG (Pierce). The capture and detection antibody pair that was used to detect $A\beta_{40}$ from cell supernatants consists of affinity purified p $A\beta_{40}$ (Invitrogen) and biotinylated 6E10 (Covance), respectively. Conditioned media was incubated with capture antibody overnight at 4 °C, followed by washing. The detecting antibody incubation was for 3 h at 4 °C, again followed by the wash steps as described previously. The plate was developed using Delfia reagents (Streptavidin–Europium and Enhancement solution (Perkin-Elmer)) and time-resolved fluorescence was measured on an EnVision multilabel plate reader (Perkin-Elmer).

Permeability Assay. The wild-type cell line LLC-PK1 (porcine renal epithelial cells, WT-LLC-PK1) was purchased from American Type Culture Collection (ATCC, Manassass, VA, USA). Transfections of WT-LLC-PK1 cells with human MDR1 gene (hMDR1-LLC-PK1) and rat *mdr1a* gene (rMDR1a-LLC-PK1) were generated. Cells were grown in Medium 199 supplemented with 10% fetal bovine serum.²⁵ Cells were seeded onto matrigel-coated transwell filter membranes at a density of 90000 cells/well. Media change was performed on day 3. Compound incubations were performed 5–6 days post seeding. All

cultures were incubated at 37 °C in a humidified (95% relative humidity) atmosphere of 5% CO₂/95% air.

Prior to the transport experiment,²⁶ culture medium was aspirated from both apical and basolateral wells, and cells were rinsed with warmed (37 °C) Hank's balanced salt solution supplemented with 10 mM Hepes at pH 7.4 (HHBSS, Invitrogen, Grand Island, NY). HHBSS was removed from wells prior to dosing with test drugs at 5 μM in transport buffer (HHBSS containing 0.1% bovine serum albumin). Then 150 μL of transport buffer were added to receiver chambers prior to dosing in triplicate to apical or basolateral chambers. The dosed transwell plates containing the cell monolayers were incubated for 2 h at 37 °C on a shaking platform. At the end of the incubation period, 100 μL samples were collected from receiver reservoirs and analyzed by LC-MS/MS on an API4000 (Applied Biosystem, Foster City, CA) triple quadrupole mass spectrometer interfaced with turbo IonSpray operated in positive mode using Analyst 1.4.2 software.

The apparent permeability coefficient (P_{app}) of all tested agents was estimated from the slope of a plot of cumulative amount of the agent versus time based on the following equation:

$$P_{app} = (dQ/dt)/(AC_0)$$

where dQ/dt is the penetration rate of the agent (ng/s), A is the surface area of the cell layer on the Transwell (0.11 cm²), and C_0 is the initial concentration of the test compound (ng/mL). Efflux ratio (ER) was calculated from the basolateral-to-apical permeability divided by the apical-to-basolateral permeability: $ER = P_{app} B > A/P_{app} A > B$.

X-Ray Crystal Structure. Recombinant human BACE1 residues 14–453 was overexpressed in bacteria as inclusion bodies and refolded using a procedure described by Patel et al.⁵ Crystals were grown in similar conditions described in Patel et al.²⁷ BACE1 protein was concentrated to 8 mg/mL in a buffer containing 20 mM Tris (pH 8.2), 150 mM NaCl, and 1 mM DTT. DMSO (3% v/v) was added to the protein immediately prior to crystallization. Apo crystals of BACE1 were grown at 20 °C using the hanging drop method/vapor diffusion method, and the drops contained 1 μL of BACE1 solution and 1 μL of reservoir solution. The reservoir solution consisted of 20% (w/v) PEG 5000 monomethylethyl ether (MME), 200 mM sodium citrate (pH 6.6), and 200 mM sodium iodide. Apo BACE1 crystal was soaked overnight in a 5.0 mM compound solution with 33% (w/v) PEG 5000 monomethylethyl ether (MME), 110 mM sodium citrate, 220 mM sodium iodide, and 10% DMSO (from compound dilution). The following day, the crystal was briefly transferred to a cryoprotectant (5.0 mM compound with 33% (w/v) PEG 5000 monomethylethyl ether (MME), 110 mM sodium citrate, 220 mM sodium iodide, 10% DMSO, and 22% glycerol) and flash frozen in liquid nitrogen. Data was collected at Advanced Light Source Beamline 5.0.2 (Lawrence Berkeley National Laboratory, Berkeley, CA, USA) at 100 K. Data was processed and scaled using HKL2000.²⁸ The crystals belong to the space group $P6_122$ with approximate unit cell dimensions of $a = 103.694$, $b = 103.694$ Å, $c = 168.866$ Å. Molecular replacement was performed using Phaser,²⁹ using an apo BACE1 structure (PDB entry 1w50) as a search model. The structure was refined using Refmac 5,³⁰ and the model with ligand was built with Coot.³¹

Pharmacodynamic Assay. Male Sprague–Dawley rats (175–200 g) were purchased from Harlan and were maintained on a 12 h light/dark cycle with unrestricted access to food and water until use. Rats were dosed orally with 17 and 21 in 2% HPMC, 1% Tween at pH 2.2. Rats were euthanized with CO₂ inhalation for 2 min, and the cisterna magna was quickly exposed by removing the skin and muscle above it. CSF (50–100 μL) was collected with a 30 gauge needle through the dura membrane covering the cisterna magna. Blood was withdrawn by cardiac puncture and plasma obtained by centrifugation for drug exposures. Brains were removed and, along with the CSF, immediately frozen on dry ice and stored at –80 °C until use. The frozen brains were subsequently homogenized in 10 volumes of (w/v) of 0.5% Triton X-100 in TBS with protease inhibitors. The homogenates were centrifuged at 100000 rpm for 30 min at 4 °C. The supernatants were analyzed for Aβ40 levels by immunoassay as follows: Meso Scale 96-

well avidin plates were coated with Biotin-4G8 (Covance) and detected with ruthenium-labeled Fab specific for Aβ40. Plates were read in MSD Sector6000 imager according to manufacturer's recommended protocol (Meso Scale Discovery, Inc.). Aβ40 concentrations were plotted using Graphpad Prism and analyzed by one-way ANOVA followed by Dunnett's multiple comparison analysis to compare drug-treated animals to vehicle-treated controls.

Chemistry. Unless otherwise noted, all materials were obtained from commercial suppliers and used without further purification. Anhydrous solvents were obtained from Aldrich or EM Science and used directly. All reactions involving air- or moisture-sensitive reagents were performed under a nitrogen or argon atmosphere. All microwave assisted reactions were conducted with a Smith synthesizer from Personal Chemistry, Uppsala, Sweden. Silica gel chromatography was performed using either glass columns packed with silica gel (230–400 mesh, EMD Chemicals, Gibbstown, NJ, USA) or prepacked silica gel cartridges (Biotage or ISCO). ¹H NMR spectra were recorded on a Bruker AV-400 (400 MHz) spectrometer at ambient temperature or on a Varian 400 MHz spectrometer. Chemical shifts are reported in parts per million (ppm, δ units) downfield from tetramethylsilane. Data are reported as follows: chemical shift, multiplicity (s = singlet, d = doublet, t = triplet, q = quartet, br = broad, m = multiplet), coupling constants, and number of protons. Purity for final compounds was greater than 95% unless otherwise noted and was measured using Agilent 1100 series high performance liquid chromatography (HPLC) systems with UV detection at 254 nm (system A, Agilent Zorbax Eclipse XDB-C8 4.6 mm × 150 mm, 5 μm, 5–100% CH₃CN in H₂O with 0.1% TFA for 15 min at 1.5 mL/min; system B, Waters Xterra 4.6 mm × 150 mm, 3.5 μm, 5–95% CH₃CN in H₂O with 0.1% TFA for 15 min at 1.0 mL/min). Exact mass confirmation was performed on an Agilent 1100 series high performance liquid chromatography (HPLC) system (Santa Clara, CA, USA) by flow injection analysis, eluting with a binary solvent system A and B (A, water with 0.1% FA; B, ACN with 0.1% FA) under isocratic conditions (50% A/50% B) at 0.2 mL/min with MS detection by an Agilent G1969A time-of-flight (TOF) mass spectrometer (Santa Clara, CA, USA).

(S)-N-((2S,3S)-1-(Benzo[d][1,3]dioxol-5-yl)-3,4-bis(tert-butylidimethylsilyloxy)butan-2-yl)-2-methylpropane-2-sulfonamide (5a). A 500 mL flask charged with (S,Z)-N-((S)-2,3-bis(tert-butylidimethylsilyloxy)propylidene)-2-methylpropane-2-sulfonamide (2.50 g, 5.93 mmol) and tetramethylethylene diamine (2.75 g, 23.6 mmol) was cooled to –78 °C and treated with a solution of 3,4-dimethoxybenzylmagnesium chloride (2.5 g, 11.9 mmol). The reaction mixture was allowed to warm to ambient temperature and stir overnight. The reaction mixture was cooled to 10 °C, and saturated NH₄Cl (50 L) and H₂O (50 mL) were added. The layers were separated, and the aqueous layer was extracted with EtOAc (2 × 100 mL). The organics were combined, dried over MgSO₄, filtered, and concentrated. The derived residue was purified by silica gel chromatography (0–25% EtOAc in hexanes) to give (S)-N-((2S,3S)-1-(benzo[d][1,3]dioxol-5-yl)-3,4-bis(tert-butylidimethylsilyloxy)butan-2-yl)-2-methylpropane-2-sulfonamide (1.44 g, 42% yield) as a colorless oil. ¹H NMR (400 MHz, CDCl₃-d) δ 6.77 (d, $J = 8.46$, 1 H), 6.69–6.71 (m, 2 H), 4.12–4.16 (m, 1 H), 3.86 (s, 3 H), 3.85 (s, 3 H), 3.74–3.76 (m, 1 H), 3.54–3.68 (m, 3 H), 2.87 (dd, $J = 14.15$, 4.42 Hz, 1 H), 2.59 (dd, $J = 14.27$, 10.11 Hz, 1 H), 0.99 (s, 9 H), 0.94 (s, 9 H), 0.93 (s, 9 H), 0.17 (s, 3 H), 0.10 (s, 6 H), 0.09 (s, 3 H). MS, $m/z = 574.3$ [M + H]⁺. Calcd for C₂₈H₅₆NO₃SSi₂: 574.2.

(S)-N-((2S,3S)-1-(Benzo[d][1,3]dioxol-5-yl)-3,4-bis(tert-butylidimethylsilyloxy)butan-2-yl)-2-methylpropane-2-sulfonamide (5b). A 2 L flask equipped with an addition funnel was charged with 15.0 g (586 mmol) of magnesium metal and 200 mL of THF. The resulting slurry was cooled to 0 °C, and a solution of 4-(chloromethyl)benzo[d][1,3]dioxole (100.0 g, 586 mmol) in 600 mL of dry THF was added dropwise such that the internal temperature did not exceed 5 °C (~1 h). A separate 3-neck 5 L flask equipped with a mechanical stirrer and addition funnel was charged with (S,Z)-N-((S)-2,3-bis(tert-butylidimethylsilyloxy)propylidene)-2-methylpropane-2-sulfonamide (123.5 g, 293 mmol) in 1.0 L of THF. The mixture was cooled to –70 °C, and a solution of the derived Grignard reagent was

added via addition funnel, keeping the internal temperature $<-65^{\circ}\text{C}$ (~ 1 h). The reaction mixture was allowed to warm to ambient temperature and stir overnight. The reaction mixture was cooled to 10°C , and saturated NH_4Cl (2.4 L) and H_2O (300 mL) were added. The layers were separated, and the aqueous layer was extracted with EtOAc (2×2.5 L). The organics were combined, dried over MgSO_4 , filtered, and concentrated. The derived residue was purified by silica gel chromatography (0–25% EtOAc in hexanes) to give (S)-N-((2S,3S)-1-(benzo[d][1,3]dioxol-5-yl)-3,4-bis(*tert*-butyldimethylsilyloxy)butan-2-yl)-2-methylpropane-2-sulfonamide (153.4 g, 76% yield) as a colorless oil. $^1\text{H NMR}$ (400 MHz, CDCl_3 -*d*) δ 6.73 (d, $J = 7.81$, 1 H), 6.70 (s, 1 H), 6.65 (d, $J = 7.73$, 1 H), 5.93 (dd, $J = 7.81$, 1.20 Hz, 2 H), 3.71 (dt, $J = 10.61$, 4.7 Hz, 1 H), 3.47–3.63 (m, 3 H), 3.39 (dd, $J = 9.55$, 5.2 Hz, 1 H), 3.20 (dd, $J = 14.02$, 4.7 Hz, 1 H), 2.81 (dd, $J = 14.01$, 10.7 Hz, 1 H), 1.22 (s, 9 H), 0.92 (s, 9 H), 0.84 (s, 9 H), 0.09 (s, 3 H), 0.04 (s, 3 H), -0.01 (s, 3 H), -0.06 (s, 3 H). MS, $m/z = 558.2$ [$\text{M} + \text{H}$] $^+$. Calcd for $\text{C}_{27}\text{H}_{52}\text{NO}_5\text{Si}_2$: 558.3.

***tert*-Butyl (2S,3S)-3-(*tert*-butyldimethylsilyloxy)-1-(3,4-dimethoxyphenyl)-4-hydroxybutan-2-ylcarbamate (6a).** To a slurry of (S)-N-((2S,3S)-3,4-bis(*tert*-butyldimethylsilyloxy)-1-(3,4-dimethoxyphenyl)butan-2-yl)-2-methylpropane-2-sulfonamide (5a, 1.35 g, 2.35 mmol) in 20 mL of ethanol at 0°C was added a solution of HCl (4 N in dioxane; 2.35 mL, 9.4 mmol). The mixture was maintained at 0°C for 5 h before being allowed to warm to rt. TEA (1.64 mL, 11.8 mmol) was added, resulting in the formation of a thick white mixture. Dichloromethane (50 mL) was added followed by Boc anhydride (1.02 g, 4.7 mmol). The resulting solution was allowed to stir at ambient temperature overnight. The reaction was quenched with saturated NH_4Cl (50 mL), and the organics were removed in vacuo. The mixture was diluted with dichloromethane (100 mL), and the mixture was poured into a separatory funnel containing water (100 mL). The layers were separated, and the aqueous layer was extracted with dichloromethane (2×100 mL). The combined organic layers were washed with brine, dried over Na_2SO_4 , filtered, and concentrated in vacuo. The derived residue was purified by silica gel chromatography (0–40% EtOAc in hexanes) to provide *tert*-butyl (2S,3S)-3-(*tert*-butyldimethylsilyloxy)-1-(3,4-dimethoxyphenyl)-4-hydroxybutan-2-ylcarbamate (6a, 785 mg, 73% yield) as a colorless oil. $^1\text{H NMR}$ (400 MHz, CDCl_3 -*d*) δ 6.69 (d, $J = 7.93$, 1), 6.54–3.67 (m, 2 H), 4.64 (d, $J = 8.01$ Hz, 1 H), 3.80–3.89 (m, 1 H), 3.74 (s, 3 H), 3.72 (s, 3 H), 3.60 (dd, $J = 9.17$, 4.7 Hz, 2 H), 3.57 (dd, $J = 12.76$, 4.4 Hz, 1 H), 2.85 (dd, $J = 12.99$, 4.4 Hz, 1 H), 2.40–2.67 (m, 2 H), 1.28 (s, 9 H), 0.92 (s, 9 H), 0.11 (s, 6 H). MS, $m/z = 456.2$ [$\text{M} + \text{H}$] $^+$. Calcd for $\text{C}_{23}\text{H}_{42}\text{NO}_6\text{Si}$: 456.2.

***tert*-Butyl (2S,3S)-1-(Benzo[d][1,3]dioxol-5-yl)-3-(*tert*-butyldimethylsilyloxy)-4-hydroxybutan-2-ylcarbamate (6b).** To a slurry of N-((2S,3S)-1-(benzo[d][1,3]dioxol-5-yl)-3,4-bis(*tert*-butyldimethylsilyloxy)butan-2-yl)-2-methylpropane-2-sulfonamide (5b, 4.40 g, 8.0 mmol) in 50 mL of ethanol at 0°C was added a solution of HCl (4 N in dioxane; 12.0 mL, 47 mmol). The mixture was maintained at 0°C for 5 h before being allowed to warm to rt. TEA (8.0 mL, 55 mmol) was added, resulting in the formation of a thick white mixture. Dichloromethane (50 mL) was added followed by Boc anhydride (4.0 g, 17 mmol). The resulting solution was allowed to stir at ambient temperature overnight. The reaction was quenched with saturated NH_4Cl (200 mL), and the organics were removed in vacuo. The mixture was diluted with dichloromethane (100 mL), and the mixture was poured into a separatory funnel containing water (100 mL). The layers were separated, and the aqueous layer was extracted with dichloromethane (2×100 mL). The combined organic layers were washed with brine, dried over Na_2SO_4 , filtered, and concentrated in vacuo. The derived residue was purified by silica gel chromatography (0–40% EtOAc in hexanes) to provide 2.71 g (78% yield) of *tert*-butyl (2S,3S)-1-(benzo[d][1,3]dioxol-5-yl)-3-(*tert*-butyldimethylsilyloxy)-4-hydroxybutan-2-ylcarbamate (6b) as a colorless oil. $^1\text{H NMR}$ (400 MHz, CDCl_3 -*d*) δ 6.74 (d, $J = 8.03$, 1), 6.71 (s, 1 H), 6.65 (d, $J = 8.34$ Hz, 1 H), 5.93 (s, 2 H), 4.69 (d, $J = 8.08$ Hz, 1 H), 3.82–3.92 (m, 1 H), 3.72 (dd, $J = 9.27$, 5.3 Hz, 2 H), 3.62 (dd, $J = 13.26$, 4.2 Hz, 1 H), 2.91 (dd, $J = 13.94$, 4.9 Hz, 1 H), 2.66 (dd, $J = 14.13$, 9.4 Hz,

1 H), 2.48 (br s, 1 H), 1.38 (s, 9 H), 0.93 (s, 9 H), 0.11 (s, 3 H), 0.10 (s, 3 H). MS, $m/z = 440.2$ [$\text{M} + \text{H}$] $^+$. Calcd for $\text{C}_{22}\text{H}_{38}\text{NO}_6\text{Si}$: 440.2.

***tert*-Butyl (2S,3S)-3-(*tert*-butyldimethylsilyloxy)-1-(3,4-dimethoxyphenyl)-4-oxobutan-2-ylcarbamate (7a).** To a solution of *tert*-butyl (2S,3S)-3-(*tert*-butyldimethylsilyloxy)-1-(3,4-dimethoxyphenyl)-4-hydroxybutan-2-ylcarbamate (6a, 400 mg, 0.88 mmol) in 20 mL of dichloromethane was added NaHCO_3 (369 mg, 4.4 mmol) and Dess–Martin periodinane (465 mg, 1.1 mmol). After 15 min, the heterogeneous mixture was diluted with methylene chloride (5 mL), 10% aqueous NaHCO_3 (10 mL), and 10% aqueous $\text{Na}_2\text{S}_2\text{O}_3$ (10 mL). The mixture was stirred vigorously for 0.5 h before the mixture was poured into a separatory funnel. The layers were separated, and the aqueous layer was extracted with methylene chloride (3×5 mL). The combined organic layers were washed with brine, dried over Na_2SO_4 , filtered, and concentrated under reduced pressure. The derived residue was purified by silica gel chromatography (0–25% EtOAc in hexanes) to provide *tert*-butyl (2S,3S)-1-(benzo[d][1,3]dioxol-5-yl)-3-(*tert*-butyldimethylsilyloxy)-4-oxobutan-2-ylcarbamate (7a, 288 mg, 72% yield) as a colorless oil. $^1\text{H NMR}$ (400 MHz, CDCl_3 -*d*) δ 9.42 (s, 1 H), 6.80 (d, $J = 8.15$ Hz, 1 H), 6.75 (s, 1 H), 6.78 (dd, $J = 8.01$ Hz, 1 H), 3.74 (s, 3 H), 3.71 (s, 3H), 4.38 (d, $J = 7.99$ Hz, 1 H), 4.18 (s, 1 H), 2.76 (dd, $J = 13.73$, 7.3 Hz, 1 H), 2.59 (dd, $J = 12.12$, 8.1 Hz, 1 H), 1.45 (s, 9 H), 0.90 (s, 9 H), 0.00 (s, 6 H). MS, $m/z = 454.3$ [$\text{M} + \text{H}$] $^+$. Calcd for $\text{C}_{23}\text{H}_{40}\text{NO}_6\text{Si}$: 454.2.

***tert*-Butyl (2S,3S)-1-(Benzo[d][1,3]dioxol-5-yl)-3-(*tert*-butyldimethylsilyloxy)-4-oxobutan-2-ylcarbamate (7b).** To a solution of *tert*-butyl (2S,3S)-1-(benzo[d][1,3]dioxol-5-yl)-3-(*tert*-butyldimethylsilyloxy)-4-hydroxybutan-2-ylcarbamate (6b, 4.3 g, 9.8 mmol) in 200 mL of dichloromethane was added NaHCO_3 (4.1 g, 49 mmol) and Dess–Martin periodinane (4.2 g, 9.9 mmol). After 15 min, the heterogeneous mixture was diluted with methylene chloride (25 mL), 10% aqueous NaHCO_3 (100 mL), and 10% aqueous $\text{Na}_2\text{S}_2\text{O}_3$ (100 mL). The mixture was stirred vigorously for 0.5 h before the mixture was poured into a separatory funnel. The layers were separated, and the aqueous layer was extracted with methylene chloride (3×50 mL). The combined organic layers were washed with brine, dried over Na_2SO_4 , filtered, and concentrated under reduced pressure. The derived residue was purified by silica gel chromatography (0–25% EtOAc in hexanes) to provide *tert*-butyl (2S,3S)-1-(benzo[d][1,3]dioxol-5-yl)-3-(*tert*-butyldimethylsilyloxy)-4-oxobutan-2-ylcarbamate (7b, 3.89 g, 91% yield) as a colorless oil. $^1\text{H NMR}$ (400 MHz, CDCl_3 -*d*) δ 9.29 (s, 1 H), 6.62 (d, $J = 8.05$ Hz, 1 H), 6.57 (s, 1 H), 6.53 (dd, $J = 7.88$ Hz, 1 H), 5.83 (s, 2 H), 4.44 (d, $J = 8.28$ Hz, 1 H), 4.12 (s, 1 H), 2.64 (dd, $J = 14.33$, 6.7 Hz, 1 H), 2.55 (dd, $J = 13.02$, 7.8 Hz, 1 H), 1.31 (s, 9 H), 0.88 (s, 9 H), 0.00 (s, 6 H). MS, $m/z = 438.2$ [$\text{M} + \text{H}$] $^+$. Calcd for $\text{C}_{22}\text{H}_{36}\text{NO}_6\text{Si}$: 438.2.

(S)-3-(3,4-Bis(difluoromethoxy)phenyl)-2-(*tert*-butoxycarbonylamino)propanoic Acid (9a). *Step A.* To a solution of methyl 2-(*tert*-butoxycarbonyl)-2-(dimethoxyphosphoryl)acetate (2.31 g, 7.76 mmol) in 10 mL of CH_2Cl_2 at 0°C was added DBU (1.17 mL, 7.76 mmol) dropwise. To this solution was then added a solution of 3,4-bis(difluoromethoxy)benzaldehyde (1.76 g, 7.39 mmol) in 10 mL of CH_2Cl_2 dropwise over 10 min. The mixture was allowed to warm to rt, where it was maintained for 2 h before being poured into saturated ammonium chloride (100 mL). The layers were separated, and the aqueous layer was extracted with CH_2Cl_2 (50 mL). The combined organic layers were washed with brine and dried over Na_2SO_4 . Filtration and concentration under reduced pressure provided an oil that was purified by silica gel chromatography (0–50% ethyl acetate in hexanes) to provide (Z)-methyl 3-(3,4-bis(difluoromethoxy)phenyl)-2-(*tert*-butoxycarbonyl)acrylate (2.84 g, 93.9% yield) as a colorless oil that solidified upon standing. MS, $m/z = 410.2$ [$\text{M} + \text{H}$] $^+$. Calcd for $\text{C}_{17}\text{F}_4\text{H}_{20}\text{NO}_6$: 410.1.

Step B. To a slurry of (Z)-methyl 3-(3,4-bis(difluoromethoxy)phenyl)-2-(*tert*-butoxycarbonyl)acrylate (2.80 g, 6.840 mmol) in 25 mL of methanol was added (1R,2S)-2-*tert*-butyl-1-((1R,2S)-2-*tert*-butyl-2,3-dihydro-1H-isophosphindol-1-yl)-2,3-dihydro-1H-isophosphindole Rh(duanphos)COD- BF_4 (0.2327 g, 0.3420 mmol). The

mixture was purged with hydrogen gas (3 \times) and then sealed at 50 psi. After 2 h, the pressure was relieved and the mixture was concentrated in vacuo. The derived residue was purified by silica gel chromatography (0–50% ethyl acetate in hexanes) to provide (*S*)-methyl 3-(3,4-bis(difluoromethoxy)phenyl)-2-(*tert*-butoxycarbonyl)propanoate (2.695 g, 95.78% yield) as a colorless oil. MS, m/z = 412.2 [M + H]⁺. Calcd for C₁₇F₄H₂₂NO₆: 412.2.

Step C. To a solution of (*S*)-methyl 3-(3,4-bis(difluoromethoxy)phenyl)-2-(*tert*-butoxycarbonyl)propanoate (2.68 g, 7 mmol) in 20 mL of THF at 0 °C was added LiOH (0.2 M, 33 mL). After stirring for 1 h, additional LiOH (0.2 M, 33 mL) was added and stirring was continued for 30 min. The reaction was then transferred to a separatory funnel and was washed with ether (2 \times 50 mL). The aqueous layer was acidified with 2N HCl to a pH = 4 and was then extracted with ethyl acetate (3 \times 100 mL). The combined organics were washed with water and brine and dried over sodium sulfate. Filtration and concentration provided (*S*)-3-(3,4-bis(difluoromethoxy)phenyl)-2-(*tert*-butoxycarbonyl)propanoic acid (2.60 g, 100% yield) as a colorless oil that was carried on without further purification. MS, m/z = 398.1 [M + H]⁺. Calcd for C₁₆F₄H₂₀NO₆: 398.2.

(S)-2-(tert-Butoxycarbonylamino)-3-(2,3-dihydrobenzo[b][1,4]dioxin-6-yl)propanoic Acid (9b). **Step A.** A solution of methyl 2-(*tert*-butoxycarbonyl)-2-(dimethoxyphosphoryl)acetate (5.08 g, 17.1 mmol) in 15 mL of CH₂Cl₂ was cooled to 0 °C and treated with DBU (2.57 mL, 17.1 mmol). The resulting solution was allowed to stir for 15 min before a solution of 2,3-dihydrobenzo[b][1,4]dioxin-6-carbaldehyde (2.670 g, 16.3 mmol) in 30 mL of CH₂Cl₂ was added. The reaction mixture was allowed to slowly warm to room temperature overnight. The reaction mixture was quenched saturated NH₄Cl (200 mL) and poured into a separatory funnel. The layers were separated, and the organic layer was washed sequentially with saturated NaHCO₃ and brine. The solution was dried over MgSO₄, filtered, and concentrated. Purification of the crude residue by column chromatography provided (*Z*)-methyl 2-(*tert*-butoxycarbonyl)-3-(2,3-dihydrobenzo[b][1,4]dioxin-6-yl)acrylate (3.545 g, 65.0% yield) as a clear viscous oil. MS, m/z = 336.2 [M + H]⁺. Calcd for C₁₇H₂₂NO₆: 336.1.

Step B. A solution of (*Z*)-methyl 2-(*tert*-butoxycarbonyl)-3-(2,3-dihydrobenzo[b][1,4]dioxin-6-yl)acrylate (5.15 g, 15.4 mmol) and (1*R*,2*S*)-2-*tert*-butyl-1-((1*R*,2*S*)-2-*tert*-butyl-2,3-dihydro-1*H*-isophosphindol-1-yl)-2,3-dihydro-1*H*-isophosphindole Rh(duanphos)COD-BF₄ (0.104 g, 0.154 mmol) in 45 mL of MeOH was placed under 50 psi hydrogen in a pressure vessel and was allowed to stir at room temperature overnight. The resulting reaction mixture was concentrated, and the crude residue was filtered through a short plug of silica eluting with CH₂Cl₂ to provide (*S*)-methyl 2-(*tert*-butoxycarbonyl)-3-(2,3-dihydrobenzo[b][1,4]dioxin-6-yl)propanoate (4.890 g, 94.4% yield) as a clear viscous oil. MS, m/z = 338.2 [M + H]⁺. Calcd for C₁₇H₂₄NO₆: 338.2.

Step C. A solution of (*S*)-methyl 2-(*tert*-butoxycarbonyl)-3-(2,3-dihydrobenzo[b][1,4]dioxin-6-yl)propanoate (3.0 g, 8.9 mmol) in 10 mL of THF and 10 mL of MeOH was cooled to 0 °C and treated with lithium hydroxide hydrate (1.9 g, 44 mmol), followed by 1 mL of water. The reaction mixture was allowed to stir at 0 °C for 2 h before being acidified to pH 4 with 6 N HCl. The mixture was then diluted with water (25 mL) and extracted with EtOAc (3 \times 25 mL). The organics were washed with brine, dried over MgSO₄, filtered, and concentrated to provide (*S*)-2-(*tert*-butoxycarbonyl)-3-(2,3-dihydrobenzo[b][1,4]dioxin-6-yl)propanoic acid (2.930 g, 102% yield) as a pale-yellow oil. This material was used in the next step without further purification. MS, m/z = 324.2 [M + H]⁺. Calcd for C₁₆H₂₂NO₆: 324.1.

(S)-4-(3,4-Bis(difluoromethoxy)phenyl)-3-(tert-butoxycarbonylamino)-2-oxobutyl Acetate (10a). To a solution of (*S*)-3-(3,4-bis(difluoromethoxy)phenyl)-2-(*tert*-butoxycarbonyl)propanoic acid (2.60 g, 7.0 mmol) in 100 mL of THF at 0 °C was added triethylamine (1.0 mL, 7.0 mmol) and isobutyl chloroformate (0.9 mL,

7.0 mmol). After stirring for 2 h, the reaction was filtered through a plug of Celite and then recooled to 0 °C. A solution of diazomethane in ether (0.5 M, 20 mL) was slowly added, and stirring was continued for 2 h before being poured into saturated sodium bicarbonate (500 mL). The aqueous layer was extracted with ethyl acetate (3 \times 300 mL), and the combined organic layers were washed with water and then brine before being dried over Na₂SO₄. Filtration and concentration under reduced pressure provided (*S*)-*tert*-butyl 1-(3,4-bis(difluoromethoxy)phenyl)-4-diazo-3-oxobutan-2-ylcarbamate (2.84 g) as a yellow solid that was used immediately in the next step. A solution of the derived diazo ketone (2.84 g) in 100 mL of THF cooled to 0 °C was treated with HBr (33% in acetic acid; 1.0 mL, 8.0 mmol). After stirring for 10 min, potassium carbonate (1.0 g, 10 mmol) and sodium acetate (5.0 g, 65 mmol) were added. The THF was removed in vacuo, and 20 mL of DMF was introduced. Stirring was continued at rt for 30 min before the reaction was diluted with ethyl acetate (100 mL) and poured in water (300 mL). The aqueous layer was extracted with ethyl acetate (2 \times 200 mL), and the combined organic layers were washed with water and then brine and dried over Na₂SO₄. Filtration and concentration under reduced pressure provided (*S*)-4-(3,4-bis(difluoromethoxy)phenyl)-3-(*tert*-butoxycarbonyl)-2-oxobutyl acetate (2.95 g, 99% yield) as a yellow oil. This material was used in the next step without further purification. MS, m/z = 454.2 [M + H]⁺. Calcd for C₁₉F₄H₂₄NO₇: 454.1.

(S)-3-(tert-Butoxycarbonylamino)-4-(2,3-dihydrobenzo[b][1,4]dioxin-6-yl)-2-oxobutyl Acetate (10b). A solution of (*S*)-2-(*tert*-butoxycarbonylamino)-3-(2,3-dihydrobenzo[b][1,4]dioxin-6-yl)propanoic acid (2.9 g, 9.00 mmol) and DIPEA (2.0 mL, 14 mmol) in 27 mL of THF was cooled to 0 °C and treated with isobutyl chloroformate (2.0 mL, 14 mmol). The resulting solution was allowed to stir for 2 h before being filtered through a short plug of silica eluting with ether. The filtrate was concentrated to provide the corresponding mixed anhydride as a thick yellow oil. This oil was taken up in 30 mL of ether, cooled to 0 °C, and treated with a solution of diazomethane in ether (0.5 M, 27 mL). This solution was allowed to stir for 30 min before being poured into a separatory funnel containing saturated NaHCO₃ (500 mL). The layers were separated, and the aqueous layer was extracted with EtOAc (2 \times 150 mL). The combined organic layers were washed with water and brine before being dried over MgSO₄, filtered, and concentrated. Purification of the crude residue by column chromatography provided (*S*)-*tert*-butyl 4-diazo-1-(2,3-dihydrobenzo[b][1,4]dioxin-6-yl)-3-oxobutan-2-ylcarbamate (1.33 g, 42% yield) as a yellow oil. The derived diazo ketone was taken up in 15 mL of THF and was cooled to 0 °C before being treated with HBr (33% in acetic acid, 0.624 mL, 11.5 mmol). After stirring for 2 h, K₂CO₃ (5.29 g, 38.3 mmol) and NaOAc (3.14 g, 38.3 mmol) were added, followed by 10 mL of DMF. The reaction mixture was allowed to warm to room temperature and stir for an additional 2 h before being diluted with EtOAc (200 mL) and washed with brine. The organics were dried over MgSO₄, filtered, and concentrated to provide (*S*)-3-(*tert*-butoxycarbonyl)-4-(2,3-dihydrobenzo[b][1,4]dioxin-6-yl)-2-oxobutyl acetate (1.530 g, 105% yield) as a pale-yellow oil. This material was used in the next step without further purification. MS, m/z = 380.2 [M + H]⁺. Calcd for C₁₉H₂₆NO₇: 380.2.

(4S)-tert-Butyl 4-(3,4-Bis(difluoromethoxy)benzyl)-5-formyl-2,2-dimethylloxazolidine-3-carboxylate (11a). **Step A.** A 200 mL RB was charged with lithium tri-*tert*-butoxy-aluminum hydride (3.31 g, 13.0 mmol). To this was added 13 mL of THF, leading to an opaque mixture. After stirring for 5 min at rt, this mixture was cooled to –78 °C, at which point 75 mL of ethanol was added. A slurry of (*S*)-4-(3,4-bis(difluoromethoxy)phenyl)-3-(*tert*-butoxycarbonyl)-2-oxobutyl acetate (2950 mg, 6.51 mmol) in 25 mL of ethanol and 10 mL of methanol and 5 mL of THF precooled to –40 °C was added dropwise via a cannula over 10 min. This addition was followed with a 5 mL THF wash of the flask containing the ketone. After stirring for 1 h at –78 °C the reaction was quenched with 200 mL of 1 N HCl. The mixture was diluted with ethyl acetate (100 mL), and 100 mL of water the layers were separated. The organic layer was concentrated, and the aqueous layer was extracted with

ethyl acetate (2 × 200 mL). The combined organics were washed with water and brine and dried over sodium sulfate. Filtration and concentration provided (2*S*,3*S*)-4-(3,4-bis-(difluoromethoxy)phenyl)-3-(*tert*-butoxycarbonyl)-2-hydroxybutyl acetate (2.90 g, 97.9% yield) as yellow oil that began to solidify upon cooling. MS, $m/z = 456.2$ [$M + H$]⁺. Calcd for C₁₉F₄H₂₆NO₇: 456.2.

Step B. To a solution of (2*S*,3*S*)-4-(3,4-bis(difluoromethoxy)phenyl)-3-(*tert*-butoxycarbonyl)-2-hydroxybutyl acetate (2.99 g, 6.57 mmol) in 20 mL of DMF was added 2-methoxy-1-propene (3.71 mL, 39.4 mmol) followed by CSA (0.763 g, 3.28 mmol). The mixture was stirred at rt for 4 h before another 1.5 mL of methoxy propene and 200 mg of CSA were added. The reaction was stirred at rt overnight before being diluted with ethyl acetate (50 mL) and poured in saturated sodium bicarbonate (250 mL). The layers were separated, and the aqueous layer was extracted with ethyl acetate (3 × 100 mL). The combined organic layers were washed with water and then brine, dried over Na₂SO₄, and filtered. Concentration under reduced pressure provided (5*S*)-*tert*-butyl 5-(3,4-bis(difluoromethoxy)benzyl)-4-(acetoxymethyl)-2,2-dimethylpyrrolidine-1-carboxylate (3.10 g, 95.7% yield) as an orange oil that was carried on as is. MS, $m/z = 496.2$ [$M + H$]⁺. Calcd for C₂₂F₄H₃₀NO₇: 496.2.

Step C. To a solution of (5*S*)-*tert*-butyl 5-(3,4-bis(difluoromethoxy)benzyl)-4-(acetoxymethyl)-2,2-dimethylpyrrolidine-1-carboxylate (3.10 g, 6.28 mmol) in 50 mL of methanol at 0 °C was added potassium carbonate (2.60 g, 18.8 mmol). After stirring for 1 h at 0 °C, 200 mL of water and 200 mL of ethyl acetate were added. The reaction was stirred at rt for 2 h, and then the organics were removed in vacuo. The mixture was diluted with ethyl acetate (100 mL) and poured in water (50 mL). The layers were separated, and the aqueous layer was extracted with ethyl acetate (3 × 100 mL). The combined organic layers were washed with water and then brine, dried over Na₂SO₄, and filtered. Concentration under reduced pressure and purified by silica gel chromatography (0–50% ethyl acetate in hexanes) provided (5*S*)-*tert*-butyl 5-(3,4-bis(difluoromethoxy)benzyl)-4-(hydroxymethyl)-2,2-dimethylpyrrolidine-1-carboxylate (1.95 g, 68.8% yield) as a colorless oil. MS, $m/z = 454.2$ [$M + H$]⁺. Calcd for C₂₀F₄H₂₈NO₆: 454.2.

Step D. A solution of (5*S*)-*tert*-butyl 5-(3,4-bis(difluoromethoxy)benzyl)-4-(hydroxymethyl)-2,2-dimethylpyrrolidine-1-carboxylate (1.93 g, 4270 μmol) in 200 mL of CH₂Cl₂ was treated with Dess–Martin periodinane (1995 mg, 4703 μmol) and sodium bicarbonate (1796 mg, 21375 μmol). The mixture was stirred for 30 min before being diluted with CH₂Cl₂ (25 mL) and quenched with 10% aqueous NaHCO₃ and 10% Na₂S₂O₃ (250 mL). After stirring vigorously for 0.5 h, the layers were separated and the aqueous layer was extracted with CH₂Cl₂ (3 × 100 mL). The combined organic layers were washed with water and then brine, dried over Na₂SO₄, and filtered. Concentration under reduced pressure and purification by silica gel chromatography (0–50% ethyl acetate in hexanes) provided (5*S*)-*tert*-butyl 5-(3,4-bis(difluoromethoxy)benzyl)-4-formyl-2,2-dimethylpyrrolidine-1-carboxylate (1.61 mg, 83.8% yield) as a yellow oil. MS, $m/z = 452.2$ [$M + H$]⁺. Calcd for C₂₀F₄H₂₆NO₆: 452.2.

(4*S*)-*tert*-Butyl 4-((2,3-Dihydrobenzo[*b*][1,4]dioxin-6-yl)methyl)-5-formyl-2,2-dimethylloxazolidine-3-carboxylate (11b). **Step A.** A solution of (S)-3-(*tert*-butoxycarbonylamino)-4-(2,3-dihydrobenzo[*b*][1,4]dioxin-6-yl)-2-oxobutyl acetate (1.53 g, 4.00 mmol) in 40 mL of EtOH cooled to 0 °C was added dropwise via a cannula to a solution of lithium tri-*tert*-butoxyaluminum hydride (8 mL, 8 mmol) in 20 mL of EtOH cooled to –78 °C. After stirring for 2 h, the reaction was quenched with 10 mL of 1*N* HCl and diluted with EtOAc (50 mL). The organics were washed with water and brine before being dried over MgSO₄. Filtration and concentration provided a residue that was purified by column chromatography to give (2*S*,3*S*)-3-(*tert*-butoxycarbonyl)-4-(2,3-dihydrobenzo[*b*][1,4]dioxin-6-yl)-2-hydroxybutyl acetate (1.26 g, 82% yield) as a white solid. MS, $m/z = 382.2$ [$M + H$]⁺. Calcd for C₁₉H₂₈NO₇: 382.2.

Step B. A solution of (2*S*,3*S*)-3-(*tert*-butoxycarbonyl)-4-(2,3-dihydrobenzo[*b*][1,4]dioxin-6-yl)-2-hydroxybutyl acetate (1.26 g, 3.30 mmol) in 4 mL DMF was treated with CSA (0.23 g, 0.99 mmol) followed by 2,2-dimethoxypropane (1.2 mL, 9.9 mmol). The mixture was allowed to stir at room temperature overnight before an additional portion of CSA and methoxypropene were added. The mixture was allowed to stir at room temperature for an additional 2 h, at which point K₂CO₃ (1.40 g, 9.90 mmol) was added followed by 3 mL of MeOH. The reaction was maintained for 2 h before being diluted with EtOAc (50 mL) and washed with water and brine. The organics were dried over MgSO₄, filtered, and concentrated. Purification of the crude residue by column chromatography gave (4*S*,5*S*)-*tert*-butyl 4-((2,3-dihydrobenzo[*b*][1,4]dioxin-6-yl)methyl)-5-(hydroxymethyl)-2,2-dimethylloxazolidine-3-carboxylate (0.582 g, 46% yield) as a colorless oil. MS, $m/z = 380.2$ [$M + H$]⁺. Calcd for C₂₀H₃₀NO₆: 380.2.

Step C. A solution of (4*S*,5*S*)-*tert*-butyl 4-((2,3-dihydrobenzo[*b*][1,4]dioxin-6-yl)methyl)-5-(hydroxymethyl)-2,2-dimethylloxazolidine-3-carboxylate (0.582 g, 1.53 mmol) in 10 mL of DCM was treated with Dess–Martin periodinane (0.716 g, 1.69 mmol) and allowed to stir at room temperature for 1 h. The reaction mixture was treated with 1 mL of saturated NaHCO₃ solution followed by sodium thiosulfate (1.21 g, 7.67 mmol). The mixture was stirred vigorously for 1 h before being diluted with EtOAc (30 mL) and washed with saturated NaHCO₃ (50 mL) and brine. The organics were dried over MgSO₄, filtered, and concentrated. Purification of the crude residue by column chromatography provided (4*S*,5*S*)-*tert*-butyl 4-((2,3-dihydrobenzo[*b*][1,4]dioxin-6-yl)methyl)-5-formyl-2,2-dimethylloxazolidine-3-carboxylate (0.537 g, 92.8% yield) as a colorless oil. MS, $m/z = 378.2$ [$M + H$]⁺. Calcd for C₂₀H₂₈NO₆: 378.2.

(2*R*,3*S*)-3-Amino-4-(3,4-dimethoxyphenyl)-1-((*S*)-6'-neopentyl-3',4'-dihydrospiro[cyclobutane-1,2'-pyrano[2,3-*b*]pyridine]-4'-ylamino)butan-2-ol trichloride (13a). **Step A.** To a solution of *tert*-butyl (2*S*,3*S*)-3-(*tert*-butyldimethylsilyloxy)-1-(3,4-dimethoxyphenyl)-4-oxobutan-2-yl carbamate (7a, 280 mg, 0.617 mmol) and (S)-6'-neopentyl-3',4'-dihydrospiro[cyclobutane-1,2'-pyrano[2,3-*b*]pyridin]-4'-amine (7, 161 mg, 0.617 mmol) in 5 mL of CH₂Cl₂ was added trimethylorthoformate (0.54 mL, 4.93 mmol). After stirring for 20 min, NaBH(OAc)₃ (523 mg, 2.50 mmol) was added and the mixture was stirred for 1 h before being diluted with CH₂Cl₂ (5 mL) and saturated Rochelle's Salt (25 mL). After stirring vigorously for 1 h, the aqueous layer was extracted with CH₂Cl₂ (3 × 10 mL). The combined organic layers were washed with brine, dried over Na₂SO₄, and filtered. Concentration under reduced pressure provided *tert*-butyl (2*S*,3*R*)-3-(*tert*-butyldimethylsilyloxy)-1-(3,4-dimethoxyphenyl)-4-((*S*)-6'-neopentyl-3',4'-dihydrospiro[cyclobutane-1,2'-pyrano[2,3-*b*]pyridine]-4'-ylamino)butan-2-yl carbamate (431 mg, 100% yield) as a yellow foam. MS, $m/z = 698.5$ [$M + H$]⁺. Calcd for C₃₉H₆₄N₃O₆Si: 698.2. This material was carried directly into the next step without further purification.

Step B. A solution of *tert*-butyl (2*S*,3*R*)-1-(3,4-dimethoxyphenyl)-3-hydroxy-4-((*S*)-6'-neopentyl-3',4'-dihydrospiro[cyclobutane-1,2'-pyrano[2,3-*b*]pyridine]-4'-ylamino)butan-2-yl carbamate (345 mg, 0.59 mmol) was taken up in methanol (5 mL) and treated with HCl (4 M in dioxane, 3.6 mL, 9.2 mmol). The solution was heated at 55 °C for 2 h before being cooled to ambient temperature and concentrated in vacuo to provide (2*R*,3*S*)-3-amino-4-(3,4-dimethoxyphenyl)-1-((*S*)-6'-neopentyl-3',4'-dihydrospiro[cyclobutane-1,2'-pyrano[2,3-*b*]pyridine]-4'-ylamino)butan-2-ol trichloride (13a, 350 mg, 100% yield) as a pale-yellow solid. ¹H NMR (400 MHz, DMSO-*d*₆) δ 10.12 (s, 1 H), 9.55 (s, 1 H), 8.12 (d, *J* = 1.76 Hz, 1 H), 7.75 (d, *J* = 2.22 Hz, 1 H), 6.78 (d, *J* = 1.23 Hz, 1 H), 6.76 (d, *J* = 7.34 Hz, 1 H), 6.80 (d, *J* = 87.78 Hz, 1 H), 4.89–4.81 (m, 2 H), 4.54 (m, 4 H), 4.21 (d, *J* = 9.89 Hz, 1 H), 3.89 (s, 6 H), 3.19–3.51 (m, 2 H), 2.75–2.95 (m, 3 H), 2.56 (dd, *J* = 12.22, 5.87 Hz, 1 H), 2.15–2.35 (m, 3 H), 1.93–2.11 (m, 2 H), 1.71–1.79 (m, 1 H), 0.89 (s, 9 H). MS, $m/z = 483.3$ [$M + H$]⁺. Calcd for C₂₈H₄₁N₃O₄: 483.2.

(2R,3S)-3-Amino-4-(benzo[d][1,3]dioxol-5-yl)-1-((S)-6'-neopentyl-3',4'-dihydrospiro[cyclobutane-1,2'-pyrano[2,3-b]pyridine]-4'-ylamino)butan-2-ol Trichloride (13b). *Step A.* To a solution of *tert*-butyl (2*S*,3*S*)-1-(benzo[d][1,3]dioxol-5-yl)-3-(*tert*-butyldimethylsilyloxy)-4-oxobutan-2-ylcarbamate (**7b**, 3.24 g, 7.4 mmol) and (S)-6'-neopentyl-3',4'-dihydrospiro[cyclobutane-1,2'-pyrano[2,3-b]pyridin]-4'-amine (**7**, 1.93 g, 7.4 mmol) in CH₂Cl₂ was added trimethylorthoformate (6.0 mL, 54 mmol). After stirring for 20 min, NaBH(OAc)₃ (6.34 g, 30 mmol) was added and the mixture was stirred for 1 h before being diluted with CH₂Cl₂ (50 mL) and saturated Rochelle's Salt (250 mL). After stirring vigorously for 1 h, the aqueous layer was extracted with CH₂Cl₂ (3 × 100 mL). The combined organic layers were washed with brine, dried over Na₂SO₄, and filtered. Concentration under reduced pressure provided *tert*-butyl (2*S*,3*R*)-1-(benzo[d][1,3]dioxol-5-yl)-3-(*tert*-butyldimethylsilyloxy)-4-((S)-6'-neopentyl-3',4'-dihydrospiro[cyclobutane-1,2'-pyrano[2,3-b]pyridine]-4'-ylamino)butan-2-ylcarbamate (5.02 g, 99% yield) as a yellow foam. MS, *m/z* = 682.2 [M + H]⁺. Calcd for C₃₈H₆₀N₃O₆Si: 682.4. This material was carried directly into the next step without further purification.

Step B. A solution of (2*S*,3*R*)-1-(benzo[d][1,3]dioxol-5-yl)-3-(*tert*-butyldimethylsilyloxy)-4-((S)-6'-neopentyl-3',4'-dihydrospiro[cyclobutane-1,2'-pyrano[2,3-b]pyridine]-4'-ylamino)butan-2-ylcarbamate (5.02 g, 7.4 mmol) was taken up in methanol (35 mL) and treated with HCl (4 M in dioxane, 46 mL, 185 mmol). The solution was heated at 55 °C for 2 h before being cooled to ambient temperature and concentrated in vacuo to provide (2*R*,3*S*)-3-amino-4-(benzo[d][1,3]dioxol-5-yl)-1-((S)-6'-neopentyl-3',4'-dihydrospiro[cyclobutane-1,2'-pyrano[2,3-b]pyridine]-4'-ylamino)butan-2-ol trichloride (**8**, 4.16 g, 98% yield) as a pale-yellow solid. ¹H NMR (400 MHz, DMSO-*d*₆) δ 10.28 (s, 1 H), 9.60 (s, 1 H), 8.28 (d, *J* = 1.53 Hz, 1 H), 7.96 (d, *J* = 1.95 Hz, 1 H), 6.98 (d, *J* = 1.41 Hz, 1 H), 6.85 (d, *J* = 7.97 Hz, 1 H), 6.80 (dd, *J* = 8.02, 1.6 Hz, 1 H), 5.99 (s, 1 H), 5.98 (s, 1 H), 4.75–4.79 (m, 2 H), 4.68 (br s, 4 H), 4.39 (d, *J* = 10.21 Hz, 1 H), 3.41–3.51 (m, 1 H), 3.22–3.34 (m, 1 H), 2.91–3.00 (m, 1 H), 2.75–2.91 (m, 2 H), 2.67 (dd, *J* = 13.16, 6.02 Hz, 1 H), 2.37–2.48 (m, 2 H), 2.15–2.25 (m, 2 H), 1.97–2.09 (m, 2 H), 1.81–1.93 (m, 1 H), 1.68–1.79 (m, 1 H), 0.88 (s, 9 H). MS, *m/z* = 468.2 [M + H]⁺. Calcd for C₂₇H₃₈N₃O₄: 468.3.

(2R,3S)-3-Amino-4-(3,4-bis(difluoromethoxy)phenyl)-1-((S)-6'-neopentyl-3',4'-dihydrospiro[cyclobutane-1,2'-pyrano[2,3-b]pyridine]-4'-ylamino)butan-2-ol Trichloride (13c). *Step A.* To a solution of (S)-6'-neopentyl-3',4'-dihydrospiro[cyclobutane-1,2'-pyrano[2,3-b]pyridin]-4'-amine (923 mg, 3544 μmol) and (4*S*)-*tert*-butyl 4-(3,4-bis(difluoromethoxy)benzyl)-5-formyl-2,2-dimethyl-5-oxazololidine-3-carboxylate (1.60 g, 3544 μmol) in 25 mL of CH₂Cl₂ was added trimethylorthoformate (3.13 mL, 28356 μmol). The solution was stirred for 20 min before NaBH(OAc)₃ (3.00 g, 14178 μmol) was added, and the resulting slurry was stirred for an additional 2 h. The mixture was then diluted with CH₂Cl₂ (50 mL) and poured into a 1 L flask containing saturated Rochelle's salt (250 mL). After stirring vigorously for 0.5 h, the layers were separated and the aqueous layer was extracted with CH₂Cl₂ (3 × 100 mL). The combined organic layers were washed with water and then brine, dried over Na₂SO₄, and filtered to provide (4*S*,5*R*)-*tert*-butyl 4-(3,4-bis(difluoromethoxy)benzyl)-2,2-dimethyl-5-(((S)-6'-neopentyl-3',4'-dihydrospiro[cyclobutane-1,2'-pyrano[2,3-b]pyridine]-4'-ylamino)methyl)oxazololidine-3-carboxylate (2.39 g, 97% yield) as a pale-yellow oil. MS, *m/z* = 696.2 [M + H]⁺. Calcd for C₃₆F₄H₅₀N₃O₆: 696.4. This material was carried directly into the next step without further purification.

Step B. A solution of (4*S*,5*R*)-*tert*-butyl 4-(3,4-bis(difluoromethoxy)benzyl)-2,2-dimethyl-5-(((S)-6'-neopentyl-3',4'-dihydrospiro[cyclobutane-1,2'-pyrano[2,3-b]pyridine]-4'-ylamino)methyl)oxazololidine-3-carboxylate (2.39 g, 3.43 mmol) in 10 mL of methanol was treated with a solution of HCl in dioxane (4.0 M, 22 mL). The resulting yellow solution was heated at 55 °C for 20 min

before being concentrated and azeotroped twice from benzene to provide (2*R*,3*S*)-3-amino-4-(3,4-bis(difluoromethoxy)phenyl)-1-((S)-6'-neopentyl-3',4'-dihydrospiro[cyclobutane-1,2'-pyrano[2,3-b]pyridine]-4'-ylamino)butan-2-ol trichloride (2.28 mg, 100% yield) as a yellow solid. MS, *m/z* = 556.2 [M + H]⁺. Calcd for C₂₈F₄H₃₈N₃O₄: 556.3. This material was carried directly into the next step without further purification.

(2R,3S)-3-Amino-4-(2,3-dihydrobenzo[b][1,4]dioxin-6-yl)-1-((S)-6'-neopentyl-3',4'-dihydrospiro[cyclobutane-1,2'-pyrano[2,3-b]pyridine]-4'-ylamino)butan-2-ol Trichloride (13d). *Step A.* A solution of (S)-6'-neopentyl-3',4'-dihydrospiro[cyclobutane-1,2'-pyrano[2,3-b]pyridin]-4'-amine (0.37 g, 1.4 mmol) and (4*S*)-*tert*-butyl 4-((2,3-dihydrobenzo[b][1,4]dioxin-6-yl)methyl)-5-formyl-2,2-dimethyl-5-oxazololidine-3-carboxylate (0.54 g, 1.4 mmol) in 5.0 mL of CH₂Cl₂ was treated with trimethyl orthoformate (1.3 mL, 11 mmol) and allowed to stir at room temperature for 1 h. Sodium triacetoxyborohydride (1.2 g, 5.7 mmol) was added, and the reaction mixture was allowed to stir for an additional hour before being quenched with saturated NH₄Cl (100 mL) and MeOH (2 mL). The pH of the mixture was adjusted to 11 with NH₄OH, and the solution was treated with saturated Rochelle's salt solution (50 mL). After stirring for an additional hour, the reaction mixture was diluted with EtOAc (100 mL), washed with water and brine, and then dried over MgSO₄. Filtration and concentration provided a residue that was purified by column chromatography to provide (4*S*,5*R*)-*tert*-butyl 4-((2,3-dihydrobenzo[b][1,4]dioxin-6-yl)methyl)-2,2-dimethyl-5-(((S)-6'-neopentyl-3',4'-dihydrospiro[cyclobutane-1,2'-pyrano[2,3-b]pyridine]-4'-ylamino)methyl)oxazololidine-3-carboxylate (0.808 g, 91% yield) as a white solid. MS, *m/z* = 622.2 [M + H]⁺. Calcd for C₃₆H₅₂N₃O₆: 622.4.

Step B. A solution of (4*S*,5*R*)-*tert*-butyl 4-((2,3-dihydrobenzo[b][1,4]dioxin-6-yl)methyl)-2,2-dimethyl-5-(((S)-6'-neopentyl-3',4'-dihydrospiro[cyclobutane-1,2'-pyrano[2,3-b]pyridine]-4'-ylamino)methyl)oxazololidine-3-carboxylate (0.170 g, 0.3 mmol) in 5 mL of CH₂Cl₂ was treated with HCl in dioxane (4 N, 1.0 mL). The resulting yellow solution was allowed to stir at room temperature for 2 h before the reaction mixture was diluted with EtOAc (50 mL). The organic solution was then sequentially washed with 2N NaOH and brine before being dried over MgSO₄. Filtration and concentration yielded (2*R*,3*S*)-3-amino-4-(2,3-dihydrobenzo[b][1,4]dioxin-6-yl)-1-((S)-6'-neopentyl-3',4'-dihydrospiro[cyclobutane-1,2'-pyrano[2,3-b]pyridine]-4'-ylamino)butan-2-ol trichloride (0.108 g, 82% yield) as an off-white solid. MS, *m/z* = 482.2 [M + H]⁺. Calcd for C₂₈H₄₀N₃O₄: 482.3. This material was carried directly into the next step without further purification.

N-((2*S*,3*R*)-1-(3,4-Dimethoxyphenyl)-3-hydroxy-4-((S)-6'-neopentyl-3',4'-dihydrospiro[cyclobutane-1,2'-pyrano[2,3-b]pyridine]-4'-ylamino)butan-2-yl)acetamide (15). To a solution of (2*R*,3*S*)-3-amino-4-(3,4-dimethoxyphenyl)-1-((S)-6'-neopentyl-3',4'-dihydrospiro[cyclobutane-1,2'-pyrano[2,3-b]pyridine]-4'-ylamino)butan-2-ol (**13a**, 300 mg, 0.27 mmol) in DMF (3.0 mL) were sequentially added DIPEA (0.442 mL, 2.54 mmol) and *N*-acetylimidazole (56 mg, 0.51 mmol). The resulting slurry was maintained at room temperature for 10 h, at which point the organics were removed in vacuo and the derived residue was purified by silica gel chromatography (0–5% MeOH in CH₂Cl₂) to provide *N*-((2*S*,3*R*)-1-(3,4-dimethoxyphenyl)-3-hydroxy-4-((S)-6'-neopentyl-3',4'-dihydrospiro[cyclobutane-1,2'-pyrano[2,3-b]pyridine]-4'-ylamino)butan-2-yl)acetamide (**9a**, 205 mg, 54% yield) as an off-white solid. ¹H NMR (400 MHz, DMSO-*d*₆) δ 7.51 (s, 1 H), 7.47 (s, 1 H), 6.36 (d, *J* = 8.31 Hz, 1 H), 6.35 (s, 1 H), 6.28 (d, *J* = 8.21 Hz, 1 H), 4.36–4.44 (m, 1 H), 3.46–3.54 (m, 2 H), 3.62 (s, 3 H), 3.60 (s, 3 H), 2.82–2.85 (m, 4 H), 2.64 (dd, *J* = 14.14, 3.66 Hz, 1 H), 2.54 (dd, *J* = 12.44, 9.16 Hz, 1 H), 2.24 (dd, *J* = 13.07, 6.13 Hz, 1 H), 2.04–2.14 (m, 1 H), 2.04 (s, 3 H), 1.35–1.84 (m, 9 H), 0.44 (s, 9 H). LCMS (99%). HRMS (ESI⁺) calcd for [C₃₀H₄₃N₃O₅ + H]⁺, 526.3275; found, 526.3256.

***N*-(2*S*,3*R*)-1-(3,4-Bis(difluoromethoxy)phenyl)-3-hydroxy-4-((*S*)-6'-neopentyl-3',4'-dihydrospiro[cyclobutane-1,2'-pyrano[2,3-*b*]pyridine]-4'-ylamino)butan-2-yl)acetamide (16).** The title compound was prepared from amine 13c using a method analogous to the preparation of compound 15. Yield, 195 mg, 39%. ¹H NMR (400 MHz, MeOH-*d*₄) δ 8.01 (dd, *J* = 10.4, 1.61 Hz, 2 H), 7.14–7.24 (m, 2 H), 6.78 (dd, *J* = 14.7, 6.16 Hz, 2 H), 6.74 (d, *J* = 6.26 Hz, 1 H), 4.78 (dd, *J* = 10.7, 6.41 Hz, 1 H), 3.80–3.87 (m, 2 H), 3.24–3.37 (m, 3 H), 2.77 (dd, *J* = 13.3, 6.57 Hz, 1 H), 2.53–2.65 (m, 4 H), 2.32 (td, *J* = 8.00, 4.51 Hz, 1 H), 2.18–2.25 (m, 1 H), 1.98–2.20 (m, 3 H), 1.92 (s, 3 H), 1.82–1.87 (m, 1 H), 0.92 (s, 9 H). MS *m/z* = 598.2 [M + H]⁺. Calcd for C₃₀F₄H₄₀N₃O₅: 598.3. LCMS (100%). HRMS (ESI+) calcd for [C₃₀F₄H₃₉N₃O₅ + H]⁺, 598.2899; found, 598.2903.

***N*-(2*S*,3*R*)-1-(Benzo[*d*][1,3]dioxol-5-yl)-3-hydroxy-4-((*S*)-6'-neopentyl-3',4'-dihydrospiro[cyclobutane-1,2'-pyrano[2,3-*b*]pyridine]-4'-ylamino)butan-2-yl)acetamide (17).** To a solution of (2*R*,3*S*)-3-amino-4-(benzo[*d*][1,3]dioxol-5-yl)-1-((*S*)-6'-neopentyl-3',4'-dihydrospiro[cyclobutane-1,2'-pyrano[2,3-*b*]pyridine]-4'-ylamino)butan-2-yl) dichloride (13b, 276 mg, 0.48 mmol) in dichloromethane (3.0 mL) were sequentially added DIPEA (0.53 mL, 2.88 mmol) and *N*-acetylimidazole (53 mg, 0.48 mmol). The resulting slurry was maintained at room temperature for 10 h, at which point the organics were removed in vacuo and the derived residue was purified by silica gel chromatography (0–5% MeOH in CH₂Cl₂) to provide *N*-((2*S*,3*R*)-1-(benzo[*d*][1,3]dioxol-5-yl)-3-hydroxy-4-((*S*)-6'-neopentyl-3',4'-dihydrospiro[cyclobutane-1,2'-pyrano[2,3-*b*]pyridine]-4'-ylamino)butan-2-yl)acetamide (17, 176 mg, 72% yield) as an off-white solid. ¹H NMR (400 MHz, MeOH) δ 8.00 (m, 2 H), 6.61–6.79 (m, 3 H), 5.89 (s, 2 H), 4.88 (dd, *J* = 11.33, 6.13 Hz, 1 H), 3.90–4.02 (m, 2 H), 3.30–3.35 (m, 1 H), 2.97–3.15 (m, 2 H), 2.75 (dd, *J* = 13.11, 6.19 Hz, 1 H), 2.53 (s, 3H), 2.48–2.65 (m, 1 H), 2.18–2.39 (m, 3 H), 2.12 (t, *J* = 12.23 Hz, 1 H), 1.92–2.04 (m, 1 H), 1.78–1.91 (m, 6 H), 0.93 (s, 9 H). MS *m/z* = 510.2 [M + H]⁺. Calcd for C₂₉H₄₀N₃O₅: 510.3. LCMS (99%). HRMS (ESI+) calcd for [C₂₉H₃₉N₃O₅ + H]⁺, 510.2962; found, 510.2953.

***N*-(2*S*,3*R*)-1-(2,3-Dihydrobenzo[*b*][1,4]dioxin-6-yl)-3-hydroxy-4-((*S*)-6'-neopentyl-3',4'-dihydrospiro[cyclobutane-1,2'-pyrano[2,3-*b*]pyridine]-4'-ylamino)butan-2-yl)acetamide (18).** The title compound was prepared from amine 13d using a method analogous to the preparation of compound 17. Yield, 84 mg, 48%. ¹H NMR (400 MHz, MeOH) δ 7.86 (d, *J* = 1.90 Hz, 1 H), 7.79 (s, 1 H), 6.66–6.76 (m, 3 H), 6.50 (d, *J* = 7.81 Hz, 1 H), 4.17–4.26 (m, 5 H), 3.91–3.99 (m, 1 H), 3.91–3.61–3.64 (m, 1 H), 3.01 (dd, *J* = 14.2, 3.62 Hz, 1 H), 2.88 (d, *J* = 5.33 Hz, 2 H), 2.42–2.54 (m, 3 H), 2.44 (s, 3 H), 2.09–2.25 (m, 6 H), 1.74–1.80 (m, 4 H), 0.88 (s, 9 H). MS *m/z* = 524.2 [M + H]⁺. Calcd for C₃₀H₄₂N₃O₅: 524.3. LCMS (97%). HRMS (ESI+) calcd for [C₃₀H₄₁N₃O₅ + H]⁺, 524.3119; found, 524.3121.

***N*-(2*S*,3*R*)-1-(Benzo[*d*][1,3]dioxol-5-yl)-3-hydroxy-4-((*S*)-6'-neopentyl-3',4'-dihydrospiro[cyclobutane-1,2'-pyrano[2,3-*b*]pyridine]-4'-ylamino)butan-2-yl)-2-methoxyacetamide (19).** To a vial charged with 2-methoxyacetic acid (0.465 g, 5.16 mmol) were sequentially added CH₂Cl₂ (15 mL) and di(1*H*-imidazol-1-yl)methanone (0.837 g, 5.16 mmol). The reaction was maintained at ambient temperature for 10 min before being added to a separate flask containing a solution of amine 13b (2.84 g, 4.92 mmol), CH₂Cl₂ (60 mL), and DIPEA (4.29 mL, 24.6 mmol). The resulting solution was maintained at ambient temperature for 10 h before being diluted with CH₂Cl₂ (70 mL) and poured into a separatory funnel containing 1 N NaOH (150 mL). The layers were separated, and the organics were washed with brine, dried over Na₂SO₄, filtered, and concentrated. The derived residue was purified by silica gel chromatography (0–10% MeOH in CH₂Cl₂) to provide the title compound (2.05 g, 77% yield) as a white solid. ¹H NMR (400 MHz, MeOH) δ 7.99 (s, 1 H), 7.86 (s, 1 H), 6.57–6.84 (m, 3 H), 5.90 (s, 2 H), 4.84 (dd, *J* = 11.56, 6.51 Hz, 1 H), 3.94–4.09 (m, 2 H), 3.87 (d, *J* = 15.87 Hz, 1 H), 3.71 (d, *J* = 15.88 Hz, 1 H), 3.29 (s, 3 H), 3.11 (dd, *J* = 13.89, 3.41 Hz, 1 H), 3.02 (dd, *J* = 12.38, 8.97 Hz, 1 H), 2.65–2.77 (m, 2 H), 2.49–2.64 (m, 4 H), 2.25–2.37 (m, 2 H), 2.10 (t, *J* = 11.87 Hz, 1 H), 1.92–2.04 (m, 1 H), 1.79–1.93 (m, 1 H), 0.94 (s, 9 H). MS *m/z* = 540.2 [M + H]⁺.

Calcd for C₃₀H₄₂N₃O₆: 540.3. LCMS (98%). HRMS (ESI+) calcd for [C₃₀H₄₁N₃O₆ + H]⁺, 540.3068; found, 540.3058.

***N*-(2*S*,3*R*)-1-(Benzo[*d*][1,3]dioxol-5-yl)-3-hydroxy-4-((*S*)-6'-neopentyl-3',4'-dihydrospiro[cyclobutane-1,2'-pyrano[2,3-*b*]pyridine]-4'-ylamino)butan-2-yl)isobutyramide (20).** To a 25 mL flask charged with amine 13b (150 mg, 0.26 mmol) and CH₂Cl₂ (5 mL) was added DIPEA (47 μL, 0.26 mmol) followed by isobutyril chloride (27.7 mg, 0.26 mmol). The mixture was allowed to stir at rt for 1 h before being concentrated in vacuo and purified by HPLC to provide the title compound (3× TFA salt, 167 mg, 73% yield) as a white solid. ¹H NMR (400 MHz, DMSO-*d*₆) δ ppm 8.95–9.21 (s, 1 H), 7.95 (d, *J* = 1.96 Hz, 1 H), 7.83 (d, *J* = 1.76 Hz, 1 H), 7.69 (d, *J* = 8.22 Hz, 1 H), 6.74–6.84 (m, 2 H), 6.59–6.73 (m, 1 H), 5.94 (s, 2 H), 4.68–4.89 (m, 1 H), 3.72–3.93 (m, 2 H), 3.02–3.22 (m, 1 H), 2.76–2.96 (m, 2 H), 2.53–2.68 (m, 3 H), 2.41 (m, 3 H), 2.11–2.34 (m, 3 H), 1.93–2.09 (m, 2 H), 1.81–1.93 (m, 1 H), 1.66–1.81 (m, 1 H), 0.91 (d, *J* = 6.75 Hz, 3 H), 0.87 (s, 9 H), 0.81 (d, *J* = 6.85 Hz, 3 H). MS *m/z* = 538.2 [M + H]⁺. Calcd for C₃₁H₄₄N₃O₅: 538.3. LCMS (98%). HRMS (ESI+) calcd for [C₃₁H₄₃N₃O₅ + H]⁺, 538.3275; found, 538.3205.

(*R*)-*N*-(2*S*,3*R*)-1-(Benzo[*d*][1,3]dioxol-5-yl)-3-hydroxy-4-((*S*)-6'-neopentyl-3',4'-dihydrospiro[cyclobutane-1,2'-pyrano[2,3-*b*]pyridine]-4'-ylamino)butan-2-yl)-2-methoxypropanamide (21). The title compound was prepared from amine 13b using a method analogous to the preparation of compound 19. Yield, 16.1 g, 91%. ¹H NMR (400 MHz, DMSO-*d*₆) δ 7.76 (d, *J* = 2.0 Hz, 1 H), 7.66–7.71 (m, 1 H), 7.6 (d, *J* = 9.22 Hz, 1 H), 6.72–6.79 (m, 2 H), 6.63 (dd, *J* = 7.89, 1.33 Hz, 1 H), 5.92 (d, *J* = 2.65 Hz, 2 H), 4.88 (d, *J* = 5.81 Hz, 1 H), 3.89–3.99 (m, 1 H), 3.79–3.89 (m, 1 H), 3.44–3.55 (m, 2 H), 3.04 (s, 3 H), 2.97 (dd, *J* = 13.89, 3.41 Hz, 1 H), 2.58 (dd, *J* = 13.96, 10.93 Hz, 3 H), 2.27–2.41 (m, 4 H), 2.17 (t, *J* = 9.22 Hz, 1 H), 2.08 (t, *J* = 7.89 Hz, 3 H), 1.76–1.89 (m, 1 H), 1.66–1.75 (m, 1 H), 1.57–1.67 (m, 1 H), 1.07 (d, *J* = 6.69 Hz, 3 H), 0.85 (s, 9 H). MS *m/z* = 554.2 [M + H]⁺. Calcd for C₃₁H₄₄N₃O₆: 554.3. LCMS (100%). HRMS (ESI+) calcd for [C₃₁H₄₃N₃O₆ + H]⁺, 554.3225; found, 554.3214.

(*S*)-*N*-(2*S*,3*R*)-1-(Benzo[*d*][1,3]dioxol-5-yl)-3-hydroxy-4-((*S*)-6'-neopentyl-3',4'-dihydrospiro[cyclobutane-1,2'-pyrano[2,3-*b*]pyridine]-4'-ylamino)butan-2-yl)tetrahydrofuran-2-carboxamide (22). The title compound was prepared from amine 13b using a method analogous to the preparation of compound 19. Yield, 1.79 g, 85%. ¹H NMR (400 MHz, DMSO-*d*₆) δ 7.77 (s, 1 H), 7.68 (s, 1 H), 7.56 (d, *J* = 9.59 Hz, 1 H), 6.70–6.81 (m, 2 H), 6.62 (d, *J* = 8.02 Hz, 1 H), 5.94 (s, 2 H), 4.88 (d, *J* = 5.58 Hz, 1 H), 4.04 (dd, *J* = 8.12, 4.79 Hz, 1 H), 3.82–3.98 (m, 2 H), 3.73–3.82 (m, 1 H), 3.65–3.74 (m, 1 H), 3.47–3.59 (m, 1 H), 2.92 (dd, *J* = 14.18, 3.91 Hz, 1 H), 2.56–2.68 (m, 3 H), 2.27–2.42 (m, 4 H), 2.14–2.25 (m, 1 H), 1.93–2.13 (m, 4 H), 1.60–1.90 (m, 6 H), 0.86 (s, 9 H). MS *m/z* = 566.4 [M + H]⁺. Calcd for C₃₂H₄₄N₃O₆: 566.3. LCMS (99%). HRMS (ESI+) calcd for [C₃₂H₄₃N₃O₆ + H]⁺, 566.3225; found, 566.3214.

(*R*)-*N*-(2*S*,3*R*)-1-(Benzo[*d*][1,3]dioxol-5-yl)-3-hydroxy-4-((*S*)-6'-neopentyl-3',4'-dihydrospiro[cyclobutane-1,2'-pyrano[2,3-*b*]pyridine]-4'-ylamino)butan-2-yl)-2-fluoropropanamide (23). The title compound was prepared from amine 13b using a method analogous to the preparation of compound 19. Yield, 38 mg, 74%. ¹H NMR (400 MHz, DMSO-*d*₆) δ 7.83 (dd, *J* = 9.34, 1.71 Hz, 1 H), 7.77 (d, *J* = 2.25 Hz, 1 H), 7.67 (d, *J* = 1.86 Hz, 1 H), 6.77 (d, *J* = 7.92 Hz, 1 H), 6.74 (d, *J* = 1.56 Hz, 1 H), 6.64 (dd, *J* = 7.87, 1.61 Hz, 1 H), 5.93 (d, *J* = 4.01 Hz, 2 H), 4.92 (d, *J* = 5.67 Hz, 1 H), 4.80 (dq, *J* = 49.3, 6.56 Hz, 1 H), 3.91–4.01 (m, 1 H), 3.81–3.91 (m, 1 H), 3.58 (quin, *J* = 5.80 Hz, 1 H), 2.96 (dd, *J* = 13.55, 3.67 Hz, 1 H), 2.58–2.66 (m, 3 H), 2.28–2.41 (m, 4 H), 2.15–2.25 (m, 1 H), 2.10 (t, *J* = 7.97 Hz, 2 H), 1.97–2.06 (m, 1 H), 1.77–1.89 (m, 1 H), 1.59–1.77 (m, 2 H), 1.19 (dd, *J* = 24.45, 6.65 Hz, 3 H), 0.86 (s, 9 H). MS *m/z* = 542.4 [M + H]⁺. Calcd for C₃₀FH₄₁N₃O₅: 542.3. LCMS (99%). HRMS (ESI+) calcd for [C₃₀FH₄₀N₃O₅ + H]⁺, 542.3025; found, 542.3017.

***N*-(2*S*,3*R*)-1-(Benzo[*d*][1,3]dioxol-5-yl)-3-hydroxy-4-((*S*)-6'-neopentyl-3',4'-dihydrospiro[cyclobutane-1,2'-pyrano[2,3-*b*]pyridine]-4'-ylamino)butan-2-yl)-2-fluorobenzamide (24).** A solution of amine 13b (150 mg, 0.26 mmol) in CH₂Cl₂ (5 mL) was treated sequentially with HATU (99 mg, 0.26 mmol), 2-fluorobenzoic

acid (36 mg, 0.26 mmol), and DIPEA (0.23 mL, 1.30 mmol). The reaction was maintained at ambient temperature for 3 h before being quenched with 0.1 mL of 5 N HCl. The mixture was concentrated to dryness and purified by HPLC to provide the title compound (75 mg, 35% yield) as a white solid. ¹H NMR (400 MHz, DMSO-*d*₆) δ 8.17 (d, *J* = 9.29 Hz, 1 H), 7.96 (d, *J* = 1.96 Hz, 1 H), 7.83 (d, *J* = 2.05 Hz, 1 H), 7.46–7.56 (m, 1 H), 7.40 (td, *J* = 7.48, 1.76 Hz, 1 H), 7.20–7.31 (m, 2 H), 6.78–6.90 (m, 2 H), 6.73 (dd, *J* = 7.92, 1.57 Hz, 1 H), 5.96 (s, 2 H), 5.83 (br s, 1 H), 4.68–4.85 (m, 1 H), 4.05–4.19 (m, 1 H), 3.95–4.06 (m, 1 H), 3.16–3.32 (m, 1 H), 2.98 (dd, *J* = 13.60, 3.52 Hz, 2 H), 2.70 (dd, *J* = 14.08, 10.47 Hz, 1 H), 2.60 (dd, *J* = 13.84, 6.80 Hz, 1 H), 2.35–2.46 (m, 3 H), 2.11–2.27 (m, 3 H), 1.96–2.09 (m, 2 H), 1.80–1.94 (m, 1 H), 1.66–1.80 (m, 1 H), 0.86 (s, 9 H). MS *m/z* = 590.4 [M + H]⁺. Calcd for C₃₄FH₄₁N₃O₅: 590.3. LCMS (100%). HRMS (ESI+) calcd for [C₃₄FH₄₀N₃O₅ + H]⁺, 590.3025; found, 590.3015.

N-((2S,3R)-1-(Benzo[d][1,3]dioxol-5-yl)-3-hydroxy-4-((S)-6'-neopentyl-3',4'-dihydrospiro[cyclobutane-1,2'-pyrano[2,3-b]pyridine]-4'-ylamino)butan-2-yl)-2-fluoronicotinamide (25). The title compound was prepared from amine **13b** using a method analogous to the preparation of compound **24**. Yield, 125 mg, 39%. ¹H NMR (400 MHz, CDCl₃-*d*) δ 10.14 (br s, 2 H), 8.91 (s, 1 H), 8.26 (d, *J* = 17.94 Hz, 2 H), 7.88–8.13 (m, 1 H), 7.52 (s, 1 H), 6.56–6.82 (m, 3 H), 5.88 (s, 2 H), 5.00–5.20 (m, 1 H), 4.39 (dd, *J* = 7.58, 5.43 Hz, 2 H), 3.35–3.54 (m, 1 H), 2.77–3.21 (m, 6 H), 2.13–2.77 (m, 7 H), 1.93–2.07 (m, 1 H), 1.74–1.93 (m, 1 H), 0.92 (s, 9 H). MS *m/z* = 591.1 [M + H]⁺. Calcd for C₃₃FH₄₀N₄O₅: 591.3. LCMS (99%). HRMS (ESI+) calcd for [C₃₃FH₃₉N₄O₅ + H]⁺, 591.2977; found, 591.2968.

N-((2S,3R)-1-(Benzo[d][1,3]dioxol-5-yl)-3-hydroxy-4-((S)-6'-neopentyl-3',4'-dihydrospiro[cyclobutane-1,2'-pyrano[2,3-b]pyridine]-4'-ylamino)butan-2-yl)nicotinamide (26). The title compound was prepared from amine **13b** using a method analogous to the preparation of compound **24**. Yield, 119 mg, 53%. ¹H NMR (400 MHz, DMSO-*d*₆) δ 9.11 (br s, 2 H), 8.93 (d, *J* = 2.25 Hz, 1 H), 8.71 (dd, *J* = 4.84, 1.61 Hz, 1 H), 8.48 (d, *J* = 8.90 Hz, 1 H), 8.11 (dt, *J* = 8.00, 1.92 Hz, 1 H), 7.95 (d, *J* = 2.05 Hz, 1 H), 7.84 (s, 1 H), 7.52 (dd, *J* = 8.56, 4.94 Hz, 1 H), 6.86 (d, *J* = 1.47 Hz, 1 H), 6.71–6.82 (m, 2 H), 5.93 (s, 2 H), 4.72–4.82 (m, 2 H), 4.09–4.19 (m, 1 H), 4.01–4.09 (m, 1 H), 3.23–3.33 (m, 1 H), 2.99 (dd, *J* = 14.38, 3.52 Hz, 2 H), 2.77 (dd, *J* = 13.99, 10.86 Hz, 1 H), 2.63 (dd, *J* = 12.86, 6.31 Hz, 1 H), 2.36–2.47 (m, 4 H), 2.13–2.27 (m, 2 H), 1.97–2.11 (m, 2 H), 1.82–1.95 (m, 1 H), 1.69–1.79 (m, 1 H), 0.85 (s, 9 H). MS *m/z* = 573.2 [M + H]⁺. Calcd for C₃₃H₄₁N₄O₅: 573.3. LCMS (99%). HRMS (ESI+) calcd for [C₃₃H₄₀N₄O₅ + H]⁺, 573.3071; found, 573.3102.

N-((2S,3R)-1-(Benzo[d][1,3]dioxol-5-yl)-3-hydroxy-4-((S)-6'-neopentyl-3',4'-dihydrospiro[cyclobutane-1,2'-pyrano[2,3-b]pyridine]-4'-ylamino)butan-2-yl)-6-fluoronicotinamide (27). The title compound was prepared from amine **13b** using a method analogous to the preparation of compound **24** to provide the title compound as a tris TFA salt. Yield, 162 mg, 66%. ¹H NMR (400 MHz, DMSO-*d*₆) δ ¹H NMR (400 MHz, DMSO-*d*₆) δ ppm 9.10 (br s, 2 H), 8.61 (d, *J* = 2.45 Hz, 1 H), 8.49 (d, *J* = 8.41 Hz, 1 H), 8.29 (td, *J* = 8.22, 2.45 Hz, 1 H), 8.03–8.09 (m, 1 H), 7.95 (d, *J* = 1.96 Hz, 1 H), 7.82 (d, *J* = 1.96 Hz, 1 H), 7.30 (dd, *J* = 8.61, 2.54 Hz, 1 H), 6.85 (d, *J* = 1.56 Hz, 1 H), 6.71–6.80 (m, 2 H), 5.93 (s, 3 H), 4.71–4.82 (m, 1 H), 3.99–4.18 (m, 2 H), 3.21–3.31 (m, 1 H), 2.92–3.03 (m, 2 H), 2.74 (dd, *J* = 13.69, 10.66 Hz, 1 H), 2.62 (dd, *J* = 13.01, 6.16 Hz, 1 H), 2.31–2.46 (m, 3 H), 2.11–2.27 (m, 1 H), 1.95–2.10 (m, 1 H), 1.81–1.94 (m, 1 H), 1.61–1.81 (m, 1 H), 0.85 (s, 9 H). MS *m/z* = 591.3 [M + H]⁺. Calcd for C₃₃FH₄₀N₄O₅: 591.3. LCMS (98%). HRMS (ESI+) calcd for [C₃₃FH₃₉N₄O₅ + H]⁺, 591.2977; found, 591.2999.

■ ASSOCIATED CONTENT

Supporting Information

Experimental section; coordinates for co-crystal of BACE1 + compound **21**. This material is available free of charge via the Internet at <http://pubs.acs.org>.

Accession Codes

The PDB accession code for the X-ray cocrystal of BACE1 + compound **21** is 4DH6.

■ AUTHOR INFORMATION

Corresponding Author

*Phone: 617-444-5188. Fax: 617-621-3908. E-mail: mmweiss@amgen.com.

Present Addresses

[#]Eli Lilly and Company, Lilly Corporate Center, Indianapolis, Indiana 46285, United States.

[▽]Envoy Therapeutics, 555 Heritage Drive, Jupiter, Florida 33458, United States.

[○]Sanofi-Aventis, 270 Albany Street, Cambridge, Massachusetts 02139, United States.

Notes

The authors declare no competing financial interest.

■ ACKNOWLEDGMENTS

We thank Larry Miller for analytical support. We also thank Douglas Whittington for generating crystallographic figures presented in the manuscript. The Advanced Light Source is supported by the U.S. Department of Energy under contract no. DE-AC02-05CH11231.

■ ABBREVIATIONS USED

AD, Alzheimer's disease; Aβ, β-amyloid; HEA, hydroxyethyl amine; APP, amyloid precursor protein; BACE1, β-site APP cleaving enzyme; Pgp, P-glycoprotein

■ REFERENCES

- (1) (a) Alzheimer's Association. Alzheimer's disease facts and figures. *Alzheimer's Dementia* **2010**, *6*, 158–194. (b) Selkoe, D. J. Translating cell biology into therapeutic advances in Alzheimer's disease. *Nature* **1999**, *399* (Suppl. 6738), A23–A31. (c) Cummings, J. L. Alzheimer's Disease. *N. Engl. J. Med.* **2004**, *351*, 56–67. (d) Querfurth, H. W.; LaFerla, F. M. Alzheimer's Disease. *N. Engl. J. Med.* **2010**, *362*, 329–344. (e) Blennow, K.; de Leon, M. J.; Zetterberg, H. Alzheimer's disease. *Lancet* **2006**, *368*, 387–403. (f) Williams, M. Progress in Alzheimer's disease drug discovery: an update. *Curr. Opin. Invest. Drugs* **2009**, *10*, 23–34.
- (2) Goedert, M.; Spillantini, M. G. A century of Alzheimer's Disease. *Science* **2006**, *314*, 777–781.
- (3) (a) Hardy, J.; Selkoe, D. J. The Amyloid Hypothesis of Alzheimer's Disease: Progress and Problems on the Road to Therapeutics. *Science* **2002**, *297*, 353–356. (b) Prasher, V. P.; Farrer, M. J.; Kessling, A. M.; Fisher, E. M. C.; West, R. J.; Barber, S. P. C.; Butler, A. C. Molecular Mapping of Iiv Alzheimer-Type Dementia in Down's Syndrome. *Ann. Neurol.* **1998**, *43*, 380–383.
- (4) (a) Vassar, R. BACE1: The β-Secretase Enzyme in Alzheimer's Disease. *J. Mol. Neurosci.* **2004**, *23* (1–2), 105–114. (b) Sinha, S.; Lieberburg, I. Cellular mechanisms of β-amyloid production and secretion. *Proc. Natl. Acad. Sci. U.S.A.* **1999**, *96*, 11049–11053. (c) Vassar, R.; Bennett, B. D.; Babu-Khan, S.; Mendiaz, E. A.; Denis, P.; Teplow, D. B.; Ross, S.; Amarante, P.; Loeloff, R.; Luo, Y.; Fisher, S.; Fuller, J.; Edenson, S.; Lile, J.; Jarosinski, M. A.; Biere, A. L.; Curran, E.; Burgess, T.; Louis, J. C.; Collins, F.; Treanor, J.; Rogers, G.; Citron, M. beta-Secretase cleavage of Alzheimer's amyloid precursor protein by the transmembrane aspartic protease bace. *Science* **1999**, *286*, 735–741.
- (5) (a) Salloway, S.; Mintzer, J.; Weiner, M. F.; Cummings, J. L. Disease-modifying therapies in Alzheimer's disease. *Alzheimer's Dementia* **2008**, *4*, 65–79. (b) Citron, M. Alzheimer's disease: strategies for disease modification. *Nature Rev. Drug Discovery* **2010**, *9*, 387–398. (c) De Strooper, B.; Vassar, R.; Golde, T. The secretases:

enzymes with therapeutic potential in Alzheimer disease. *Nature Rev. Neurol.* **2010**, *6*, 99–107. (d) Citron, M. beta-Secretase inhibition for the treatment of Alzheimer's disease—promise and challenge. *Trends Pharmacol. Sci.* **2004**, *25*, 92–97.

(6) For recent reviews and work in this area, please see the following:

(a) Karran, E.; Mercken, M.; De Strooper, B. The amyloid cascade hypothesis for Alzheimer's disease: an appraisal for the development of therapeutics. *Nature Rev. Drug Discovery* **2010**, *9*, 560–574. (b) Malamas, M. S.; Erdei, J.; Gunawan, I.; Turner, J.; Hu, Y.; Wagner, E.; Fan, K.; Chopra, R.; Olland, A.; Bard, J.; Jacobsen, S.; Magolda, R. L.; Pangalos, M.; Robichaud, A. J. Design and Synthesis of 5,5'-Disubstituted Aminohydantoin as Potent and Selective Human β -Secretase (BACE1) Inhibitors. *J. Med. Chem.* **2010**, *53*, 1146–1158. (c) Tresadern, G.; Delgado, F.; Delgado, O.; Gijzen, H.; Macdonald, G. J.; Moechars, D.; Rombouts, F.; Alexander, R.; Spurlino, J.; Gool, M. V.; Vega, J. A.; Trabanco, A. T. Rational design and synthesis of aminopiperazinones as β -secretase (BACE) inhibitors. *Bioorg. Med. Chem. Lett.* **2011**, *21*, 7255–7260. (d) Boy, K. M.; Guernon, J. M.; Shi, J.; Toyn, J. H.; Meredith, J. E.; Barten, D. M.; Burton, C. R.; Albright, C. F.; Marcinkeviciene, J.; Good, A. C.; Tebben, A. J.; Muckelbauer, J. K.; Camac, D. M.; Lentz, K. A.; Bronson, J. J.; Olson, R. E.; Macor, J. E.; Thompson, L. A., III. Monosubstituted γ -lactam and conformationally constrained 1,3-diaminopropan-2-ol transition-state isostere inhibitors of β -secretase (BACE). *Bioorg. Med. Chem. Lett.* **2011**, *21*, 6916–6924. (e) Swahn, B. M.; Holenz, J.; Kihlström, J.; Kolmodin, K.; Lindström, J.; Plobeck, N.; Rotticci, D.; Sehgelmeble, F.; Sundström, M.; von Berg, S.; Fälting, J.; Georgievska, B.; Gustavsson, S.; Neelissen, J.; Ek, M.; Olsson, L. L.; Berg, S. Aminoimidazoles as BACE-1 inhibitors: The challenge to achieve in vivo brain efficacy. *Bioorg. Med. Chem. Lett.* **2012**, *22*, 1854–1859. (f) Cumming, J. N.; Smith, E. M.; Wang, L.; Misiaszek, J.; Durkin, J.; Pan, J.; Iserloh, U.; Wu, Y.; Zhu, Z.; Strickland, C.; Voigt, J.; Chen, X.; Kennedy, M. E.; Kuvelkar, R.; Hyde, L. A.; Cox, K.; Favreau, L.; Czarniecki, M. F.; Greenlee, W. J.; McKittrick, B. A.; Parker, E. M.; Stamford, A. W. Structure based design of iminohydantoin BACE1 inhibitors: identification of an orally available, centrally active BACE1 inhibitor. *Bioorg. Med. Chem. Lett.* **2012**, *22*, 2444–2449.

(7) Kaller, M. M.; Harried, S. S.; Albrecht, B.; Amarante, P.; Babu-Khan, S.; Bartberger, M. D.; Brown, J.; Chen, K.; Cheng, Y.; Citron, M.; Croghan, M. D.; Dunn, R.; Graceffa, R.; Hickman, D.; Judd, T.; Kreiman, C.; La, D.; Lopez, P.; Luo, Y.; Masse, C.; Monenschein, H.; Nguyen, T.; Pennington, L. D.; San Miguel, T.; Wahl, R. C.; Weiss, M. M.; Wen, P. H.; Williamson, T.; Wood, S.; Xue, M.; Yang, B.; Zhang, J.; Patel, V.; Zhong, W.; Hitchcock, S. A potent and orally efficacious, hydroxyethylamine based inhibitor of beta-secretase. *Bioorg. Med. Chem. Lett.* **2012**, submitted for publication.

(8) Harried, S. S.; Croghan, M. D.; Kaller, M. R.; Lopez, P.; Zhong, W.; Hungate, R.; Reider, P. J. Stereoselective synthesis of anti-N-protected 3-amino-1,2-epoxides by nucleophilic addition to *N*-tert-butanesulfonyl imine of a glyceraldehydes synthon. *J. Org. Chem.* **2009**, *74* (16), 5975–5982.

(9) Johnson, T. W.; Dress, K. R.; Edwards, M. Using the Golden Triangle to optimize clearance and oral absorption. *Bioorg. Med. Chem. Lett.* **2009**, *19*, 5560–5564 and references therein.

(10) Metabolite identification studies demonstrated that the primary sites of oxidative metabolism were in the neopentyl fragment.

(11) Kumagai, Y.; Fukuto, J. M.; Cho, A. K. Disposition of Methylendioxyphenyl Compounds. *Curr. Med. Chem.* **1994**, *4*, 254–261 and references therein.

(12) Murray, M. Methylendioxyphenyl insecticide synergists as potential human health hazards. *Curr. Drug Metab.* **2000**, *1*, 67–84.

(13) Koudriakova, T.; Iatsimirskaia, E.; Utkin, I.; Gangl, E.; Vouros, P.; Storozhuk, E.; Orza, D.; Marinina, J.; Gerber, N. Modulation of Drug Metabolism and Antiviral Therapies. *Drug Metab. Dispos.* **1998**, *26*, 552–561.

(14) (a) Acosta, E. P. Pharmacokinetic enhancement of protease inhibitors. *JAIDS, J. Acquired Immune Defic. Syndr.* **2002**, *29*, S11–S18. (b) Rathbun, R. C.; Rossi, D. R. Low-Dose Ritonavir for Protease Inhibitor Pharmacokinetic Enhancement. *Ann. Pharmacother.* **2002**, *36*,

702–706. (c) Kempf, D. J.; Marsh, K. C.; Kumar, G.; Rodrigues, A. D.; Denissen, J. F.; McDonald, E.; Kukulka, M. J.; Hsu, A.; Granneman, G. R.; Baroldi, P. A.; Sun, E.; Pizzuti, D.; Plattner, J. J.; Norbeck, D. W.; Leonard, J. M. Pharmacokinetic enhancement of inhibitors of the human immunodeficiency virus protease by coadministration with ritonavir. *Antimicrob. Agents Chemother.* **1997**, *41*, 654–660.

(15) HMG CoA reductase inhibitors are commonly used by the elderly population. Within this class of inhibitors, pravastatin and rosuvastatin represent two medications that are not metabolized by Cyp3A4.

(16) Mahar Doan, K. M.; Humphreys, J. E.; Webster, L. O.; Wring, S. A.; Shampine, L. J.; Serabjit-Singh, C. J.; Adkinson, K. K.; Polli, J. W. Passive permeability and P-glycoprotein mediated efflux differentiate CNS and non-CNS marketed drugs. *J. Pharmacol. Exp. Ther.* **2002**, *303*, 1029–1037.

(17) Liu, X.; Van Natta, K.; Yeo, H.; Vilenski, O.; Weller, P. E.; Worboys, P. D.; Monshouwer, M. Unbound Drug Concentration in Brain Homogenate and Cerebral Spinal Fluid at Steady State as a Surrogate for Unbound Concentration in Brain Interstitial Fluid. *Drug Metab. Dispos.* **2009**, *37*, 787–793.

(18) Hitchcock, S. A.; Pennington, L. D. Structure–Brain Exposure Relationships. *J. Med. Chem.* **2006**, *26*, 7559–7583 and references therein.

(19) Kuhn, B.; Mohr, P.; Stahl, M. Intramolecular hydrogen bonding in medicinal chemistry. *J. Med. Chem.* **2010**, *53*, 2601–2611.

(20) Coordinates for the complex of BACE with inhibitor **21** have been deposited in the Protein Data Bank under PDB 4DH6.

(21) (a) Hong, L.; Turner, R. T.; Koelsch, G.; Shin, D.; Ghosh, A. K.; Tang, J. Crystal structure of memapsin 2 (beta-secretase) in complex with an inhibitor OM00–3. *Biochemistry* **2002**, *41*, 10963–10967.

(b) Hong, L.; Tang, J. Flap position of free memapsin 2 (beta-secretase), a model for flap opening in aspartic protease catalysis. *Biochemistry* **2004**, *43*, 4689–4695.

(22) Plasma protein binding values were interpolated using best-fit parameters generated from fitting a two-site binding model.

(23) Turner, R. T., III; Koelsch, G.; Hong, L.; Castanheira, P.; Ghosh, A.; Tang, J. Subsite specificity of memapsin (β -secretase): implications for inhibitor design. *Biochemistry* **2001**, *40*, 10001–10006.

(24) Haniu, M.; Denis, P.; Young, Y.; Mendiaz, E. A.; Fuller, J.; Hui, J. O.; Bennett, B. D.; Kahn, S.; Ross, S.; Burgess, T. Characterization of Alzheimer's beta-secretase protein BACE. A pepsin family member with unusual properties. *J. Biol. Chem.* **2000**, *275*, 21099–21106.

(25) Schinkel, A. H.; Wagenaar, E.; van Deemter, L.; Mol, C. A. A. M.; Borst, P. Absence of the *mdr1a* P-glycoprotein in mice affects tissue distribution and pharmacokinetics of dexamethasone, digoxin, and cyclosporin A. *J. Clin. Invest.* **1995**, *96*, 1698–1705.

(26) Booth-Genthe, C. L.; Louie, S. W.; Carlini, E. J.; Li, B.; Leake, B. F.; Eisenhandler, R.; Hochman, J. H.; Mei, Q.; Kim, R. B.; Rushmore, T. H.; Yamazaki, M. Development and characterization of LLC-PK1 cells containing Sprague–Dawley rat *Abcb1a* (*Mdr1a*): comparison of rat P-glycoprotein transport to human and mouse. *J. Pharmacol. Toxicol. Methods* **2006**, *54*, 78–89.

(27) Patel, S.; Vuillard, L.; Cleasby, A.; Murray, C. W.; Yon, J. Apo and inhibitor complex structures of BACE (beta-secretase). *J. Mol. Biol.* **2004**, *343*, 407–416.

(28) Otwinowski, Z.; Minor, W. Processing of X-ray diffraction data collected in oscillation mode. *Methods Enzymol.* **1997**, *276*, 307–326.

(29) McCoy, A. J.; Grosse-Kunstleve, R. W.; Adams, P. D.; Winn, M. D.; Storoni, L. C.; Read, R. J. Phaser crystallographic software. *J. Appl. Crystallogr.* **2007**, *40*, 658–674.

(30) Murshudov, G. N.; Vagin, A. A.; Dodson, E. J. Refinement of macromolecular structures by the maximum-likelihood method. *Acta Crystallogr., Sect. D: Biol. Crystallogr.* **1997**, *D53*, 240–255.

(31) Emsley, P.; Cowtan, K. Coot: model-building tools for molecular graphics. *Acta Crystallogr., Sect. D: Biol. Crystallogr.* **2004**, *D60*, 2126–2132.

(32) Dineen, T. A.; Weiss, M. M.; Williamson, T.; Acton, P.; Babu-Khan, S.; Bartberger, M. D.; Brown, J.; Chen, K.; Cheng, Y.; Citron, M.; Croghan, M. D.; Dunn, R. T., II; Esmay, J.; Graceffa, R. F.;

Harried, S. S.; Hickman, D.; Hitchcock, S. A.; Horne, D. B.; Huang, H.; Imbeah-Ampiah, R.; Judd, T.; Kaller, M. R.; Kreiman, C. R.; La, D. S.; Li, V.; Lopez, P.; Louie, S.; Monenschein, H.; Nguyen, T. T.; Pennington, L. D.; San Miguel, T.; Sickmier, E. A.; Vargas, H. M.; Wahl, R. C.; Wen, P. H.; Whittington, D. A.; Wood, S.; Xue, Q.; Yang, B. H.; Patel, V. F.; Zhong, W. Design and Synthesis of Potent, Orally Efficacious Hydroxyethylamine Derived β -Site Amyloid Precursor Protein Cleaving Enzyme (BACE1) Inhibitors. *J. Med. Chem* **2012**, DOI: 10.1021/jm300118s.